

# **DISTRIBUTION SYSTEM RELIABILITY ENHANCEMENT**

A Thesis  
Presented to  
The Academic Faculty

by

Xuebei Yu

In Partial Fulfillment  
of the Requirements for the Degree  
Master of Science in the  
School of Electrical and Computer Engineering

Georgia Institute of Technology  
August 2011

**COPYRIGHT 2011 BY XUEBEI YU**

# **DISTRIBUTION SYSTEM RELIABILITY ENHANCEMENT**

Approved by:

Dr. A.P. Meliopoulos, Advisor  
School of Electrical and Computer Engineering  
*Georgia Institute of Technology*

Dr. Deepakraj M Divan  
School of Electrical and Computer Engineering  
*Georgia Institute of Technology*

Dr. Carlos S Grijalva  
School of Electrical and Computer Engineering  
*Georgia Institute of Technology*

Date Approved: May 16<sup>th</sup> 2011

## **ACKNOWLEDGEMENTS**

I would like to thank my advisor Dr. A.P. Meliopoulos for an opportunity to work on this project and his continued guidance. I would also like to thank the committee, Dr. Deepakraj M Divan and Dr. Carlos S Grijalva for their time.

During the course of my Masters, I have had the opportunity to exchange ideas with many of my fellow students, and this has helped me a great deal in my research. For this, I would like to thank Vangelis Farantatos, Ye Tao, Renke Huang, Peter Suh, Ravi Shankar, Joosung Kang and Anupama Keeli. I would particularly like to thank Renke Huang and Vangelis Farantatos for taking the time to help me during the course of my research, and also for providing many valuable pointers.

I would like to thank my parents for their love and support, this has continued to be a source of encouragement.

# TABLE OF CONTENTS

	Page
ACKNOWLEDGEMENTS	iv
LIST OF TABLES	vii
LIST OF FIGURES	ix
LIST OF SYMBOLS AND ABBREVIATIONS	xi
SUMMARY	xiii
 <u>CHAPTER</u>	
1 Introduction	1
1.2 Research Objectives Statement	1
1.2 Research Objectives	3
2 Background Information	5
2.1 System Drives	5
2.2 Power Outage Definition	5
2.3 System Indices	6
3 Initial Response	9
3.1 Introduction	9
3.2 Relays	10
3.2.1 Adaptive Relay Scheme – Directional Overcurrent Relay	11
3.2.2 Adaptive Relay Scheme – Impedance Relay	24
3.2.3 Coordination of Overcurrent Relays and Distance Relays	26
3.3 Fuse	34
3.3.1 Characteristic Parameters	35
3.3.2 Fuse Operation	37

3.4	Coordination of Relays and Fuses	39
3.5	Test System and Calculation	41
3.5.1	System Description	41
3.5.2	Problem Formulation	43
3.5.3	Solution	48
4	Automatic System Response	50
4.1	Introduction	50
4.2	Switch Placement Optimization	51
4.2.1	Problem Formulation	53
4.2.2	Particle Swarm Optimization	55
4.2.3	Genetic Algorithm	72
4.2.4	Results and Conclusions	78
4.3	Automatic Network Reconfiguration	79
4.3.1	Simple Rule-based Reconfiguration	79
4.3.2	Simulation Results of the Optimal Reconfiguration	84
5	Conclusion and Future Work	85
APPENDIX A:	Basic Reliability Calculations	87
APPENDIX B:	Description of the Test System	89
REFERENCES		99

## LIST OF TABLES

	Page
Table 3.1: Constants and exponents for standard characteristics of overcurrent relays	15
Table 3.2: Constraints of the pickup current of each relay in example system	19
Table 3.3: Fault current at each relay to different fault locations	20
Table 3.4: Results for the MINLP and LP formulation	24
Table 3.5: Fault current at each relay to 8 different fault locations	30
Table 3.6: Results for the coordination of overcurrent and distance relay setting	33
Table 3.7: Constraints of the pickup current in IEEE 123 node test system	43
Table 3.8: Fault current in IEEE 123 node test system	44
Table 3.9: Results for the optimal relay setting in IEEE 123 node system	49
Table 4.1: Number of function evaluation for continuous case	61
Table 4.2: Objective function for continuous case	62
Table 4.3: Number of function evaluation for integer case	62
Table 4.4: Objective function for integer case	62
Table 4.5: Comparison of 1-switch and 2-switch simulations	64
Table 4.6: Fval, SAIDI Reduction, & Cost of 1-Switch Verification Case	65
Table 4.7: Number of Function Evaluations of 1-Switch PSO Optimization	67
Table 4.8: Objective Function of 1-Switch PSO Optimization	67
Table 4.9: Number of Function Evaluations of 2-Switch PSO Optimization	68
Table 4.10: Objective Function of 2-Switch PSO Optimization	68
Table 4.11: Optimization Results of PSO with 10 Fault Profiles	70
Table 4.12: Objective Function, SAIDI Reduction, and Cost of 120-Switch Case	71
Table 4.13: Comparison of PSO and GA	78

Table 4.14: Optimal GA Switch Configuration Results	78
Table 4.15: Effects of Types of Switches on Reliability	84
Table B.1: Line segment data	90
Table B.2: Three Phase Switches	91
Table B.3: Overhead Line Configuratioions	91
Table B.4: Underground Line Configuration	91
Table B.5: Shunt Capacitors data	91
Table B.6: Overhead Line Spacing	92
Table B.7: Underground Line Spacing	92
Table B.8: Load data	93
Table B.9: Switch type and location in the test system	95
Table B.10: Load data in the test system	96

## LIST OF FIGURES

	Page
Figure 3.1: Example distribution system	18
Figure 3.2: Fault simulation in the example distribution system	20
Figure 3.3: Distance relay protection zone for a radial system	25
Figure 3.4: Coordination of overcurrent relays	28
Figure 3.5: Coordination of overcurrent relays and distance relays	28
Figure 3.6: Test system for coordination of overcurrent relays and distance relays	29
Figure 3.7: Minimum Melting Time and Total Clearing Time for a Specific Fuse	36
Figure 3.8: Fault time current curve	38
Figure 3.9: Time current curve for fuse 40K	39
Figure 3.10: Fuse blow scheme	40
Figure 3.11: Fuse saving scheme	40
Figure 3.12: IEEE 123-Node Test Feeder	42
Figure 3.13: IEEE 123-Node Test Feeder in WinIGS - F	43
Figure 3.14: IEEE 123-Node Test Feeder with fault simulation	44
Figure 4.1: Switch Placement Optimization	52
Figure 4.2: Contour plot of sample objective function	61
Figure 4.3: Validation of PSO Algorithm	63
Figure 4.4: Verification of PSO Algorithm with 1 Switch	69
Figure 4.5: Objective Function of 1-Switch PSO Optimization	71
Figure 4.6: SAIDI Reduction of 1-Switch PSO Optimization	72
Figure 4.7: Selection - Elitest vs. Roulette Wheel	74
Figure 4.8: Two-Point Crossover of GA	75

Figure 4.9: Mutation of GA	76
Figure 4.10: Optimal switch locations for 1 year payback period	79
Figure 4.11: Data Structure for Node 13	80
Figure 4.12: Paths finding and switch commands determination	81
Figure 4.13: Optimal switch locations for automatic reconfiguration	82
Figure 4.14: Network Plot @ $t=12s$ with a Fault at Node 19	84
Figure B.1: IEEE 123-Node Test Feeder	89
Figure B.2: Overhead Line Spacing	92
Figure B.3: Underground Line Spacing	92
Figure B.4: IEEE 123-Node Test Feeder in WinIGS - F	94

## LIST OF SYMBOLS AND ABBREVIATIONS

SAIDI	System Average Interruption Duration Index
CAIDI	Customer Average Interruption Duration Index
SAIFI	System Average Interruption Frequency Index
MAIFI	Momentary Average Interruption Frequency Index
FDIR	Fault detection, isolation and restoration
DOE	Department of Energy
TDS	Time dial setting
$I_p$	Pickup current
LP	Linear Programming
NLP	Nonlinear Programming
MINLP	Mixed Integer Nonlinear Programming
IEEE	Institute of Electrical and Electronics Engineers
WinIGS	Windows Integrated Grounding System
LINGO	Linear Interactive and General Optimizer
TCC	Time Current Curve
PSO	Particle Swarm Optimization
GA	Genetic Algorithm
FVAL	Function Value
$i$	Nearest relay to the fault $i=F(j)$
$T_{i,j}$	Operation time of relay $i$ for a fault at location $j$
$\Delta T$	Time interval between primary relay and backup relay
$I_{ij}$	Fault current at relay $i$ for a fault at place $j$ ,

$\Delta T'$	Time interval between overcurrent relay and distance relay
$T_{zi}$	Time setting for zone $i$ of distance relay
$I_N$	Rated current of fuse
$V_N$	Rated Voltage of fuse
$N_T$	Total number of customers served in an area
$x_{k+1}^i$	Position of the particle $i$ at the iteration $k+1$
$v_{k+1}^i$	Velocity of the particle $i$ at the iteration $k+1$
$p^i$	Best position found by particle $i$
$r$	Independent random numbers between 0 and 1
$w$	Weight

## SUMMARY

Practically all everyday life tasks from economic transactions to entertainment depend on the availability of electricity. Some customers have come to expect a higher level of power quality and availability from their electric utility. Federal and state standards are now mandated for power service quality and utilities may be penalized if the number of interruptions exceeds the mandated standards. In order to meet the requirement for safety, reliability and quality of supply in distribution system, adaptive relaying and optimal network reconfiguration are proposed. By optimizing the system to be better prepared to handle a fault, the end result will be that in the event of a fault, the minimum number of customers will be affected. Thus reliability will increase.

The main function of power system protection is to detect and remove the faulted parts as fast and as selectively as possible. The problem of coordinating protective relays in electric power systems consists of selecting suitable settings such that their fundamental protective function is met under the requirements of sensitivity, selectivity, reliability, and speed. In the proposed adaptive relaying approach, weather data will be incorporated as follows. By using real-time weather information, the potential area that might be affected by the severe weather will be determined. An algorithm is proposed for adaptive optimal relay setting (relays will optimally react to a potential fault). Different types of relays (and relay functions) and fuses will be considered in this optimization problem as well as their coordination with others. The proposed optimization method is based on mixed integer programming that will provide the optimal relay settings including pickup current, time dial setting, and different relay functions and so on.

The main function of optimal network reconfiguration is to maximize the power supply using existing breakers and switches in the system. The ability to quickly and flexibly reconfigure the power system of an interconnected network of feeders is a key component of Smart Grid. New technologies are being injected into the distribution systems such as advanced metering, distribution automation, distribution generation and distributed storage. With these new technologies, the optimal network reconfiguration becomes more complicated. The proposed algorithms will be implemented and demonstrated on a realistic test system. The end result will be improved reliability. The improvements will be quantified with reliability indexes such as SAIDI.

# CHAPTER 1

## INTRODUCTION

### 1.1 Problem Statement

The reliability of electric distribution systems in the US is one which can affect any business or other entity dependent on electricity for any reason. Customers deal with problems as small as a light flickers to extended outages which may take hours or even days to fix. Some businesses that lose power for even a few seconds may completely lose a product in development costing them hundreds of thousands of dollars. Outages have cost the U.S. economy an average of \$1.5 billion each week – \$80 billion each year, and customers and utilities alike are looking for a cost effective solution.

In order to improve reliability of the power system, many smart grid technologies are being and will be implemented in the distribution system. Presently, most distribution systems are designed based on a main trunk three phase feeder with single-phase laterals. The main trunk carries most power away from the substation through the center of the feeder service territory. Single phase laterals are used to connect the main trunk to customer locations. Actual distribution systems have branching, normally-open loops, and other complexities, but the overarching philosophy remains the same [1]. Traditional distribution systems use time-current coordination for protection devices. These devices assume that faster devices are topologically further from the substation.

Distribution systems will not resemble the distribution systems of today in several years. New technologies are being injected into the distribution systems such as advanced

metering, distribution automation, distribution generation and distributed storage. An example test system is built in Appendix B which includes some of the new smart grid technologies. Through the integrated use of these technologies, smart grid will be able to self heal, provide high reliability and power quality, be resistant to cyber attacks, operate with multi-directional power flow, increase equipment utilization.

A Smart Grid does not just try to connect substations to customers for the lowest cost. Instead, a Smart Grid is an enabling system that can be quickly and flexibly reconfigured. Therefore, future distribution systems will be an integrated Grid of distribution lines, with the grid being connected to multiple power sources. In a Smart Grid, topology is flexible and the assumption that faster devices are topologically further from the substation is problematic. System topology and system protection will have to be coordinated properly to ensure proper protection coordination for a variety of configurations. In order to take advantages of these changes, reengineering and optimizing the existing distribution systems is necessary. For example, adaptive relay programming is proposed to combat sustained power outages resulting from wind and lightning related weather events, and it is claimed that the SAIDI reliability metric can be improved by as much as 30% annually.

The ability to quickly and flexibly reconfigure an interconnected network of feeders is a key component of Smart Grid, and the most important aspects are in the areas of protection and switching (often integrated into the same device like breakers and reclosers). Switches (including breakers, load break switches, tie switches) play important roles in Fault Detection, Isolation and Restoration (FDIR). At a permanent

fault occurrence, the following operations are taken. 1) An automatic feeder breaker/recloser will trip in real time operation to cut off the fault from the feeder, 2) the feeders are broken up into sections isolated by switches or breakers 3) power is then restored to non faulted sections.

## **1.2 Research Objectives**

The present project addresses the above issues. We propose three specific focus areas. Two related to real time operations and the third addressing the planning issue. These are defined below.

### **Focus Area 1: Initial response**

By using real-time weather information, the potential area that might be affected by the severe weather will be determined. An algorithm will be built for adaptive relay setting for the specific configuration of the system so that the relays can optimally react to a potential fault. Different types of relays (and relay functions) and fuses will be considered in this optimization problem.

### **Focus Area 2: Sectionalization and power restoration**

An algorithm will be developed to detect the section of the feeder with fault occurred, quickly isolate that feeder section by operating the isolating switches or breakers and restoring power to the non faulted sections. The objective is to maximum power supply to customers considering the existed smart grid technologies such as distributed energy resources and distribution automation devices.

### Focus Area 3: Switch Placement Optimization

It is obvious that adding more switches in the power system can improve power system reliability. There exists a trade-off between power reliability improvements and switch costs. Therefore, several algorithms are built to decide the optimal number of switches added to the system and the best locations to add those switches.

## **CHAPTER 2**

### **BACKGROUND AND LITERATURE REVIEW**

#### **2.1 Reliability in Power System**

##### **2.1.1 System Drives**

With today's high electricity costs, customers have come to expect a higher level of power quality from their electric utility. Higher power quality requirements have become even more critical with the proliferation of electronic devices such as VCRs, computers and clock radios, which are intolerant of even the smallest interruption of power. These issues have become so important to utility customers that federal and state standards are now mandated for power quality and utilities are now penalized if the number of interruptions exceeds these mandated standards.

The primary reason for many outages is the aging of the electric grid, as well as the lack of redundancy, due to the generally centralized nature of the system. In fact, over 80% of transformers, as well as 80% of breakers are 30 years old or older (DOE). Uncontrollable events such as animal contact or human interaction on the line may also lead to power outages. Weather can be especially hazardous, sometimes causing cascading faults leading to millions of dollars of expense. Tree branches may touch lines during a storm potentially causing an outage, leading to tree trimming programs.

##### **2.1.2 Power Outage Definition**

Two types of outages may occur and can be categorized as momentary or sustained outages. A momentary outage is defined as being any outage lasting from 1 second to 1 minute. Afterwards, it is considered to be a sustained outage. Anything less than 1 second is a power quality issue. Other definitions for momentary outages consider it to be any outage lasting less than 5 minutes. It is debatable, but the point is that an outage, however short, still affects customers and is not desired.

### **2.1.3 System Indices**

The objective of many distribution utilities today is to improve overall customer satisfaction through quality of service, which is to maximize the reliability of power distribution system. Quality of service in part is monitored through system performance indices such as Momentary Average Interruption Frequency Index (MAIFI), Sustained Average Interruption Duration Index (SAIDI), Customer Average Interruption Duration Index (CAIDI) and Sustained Average Interruption Frequency Index (SAIFI). Definition of these indices can be found in Appendix A. Utility companies are measured by these indices on a yearly basis, and in some states may receive bonuses or penalties depending on how far they are away from target values or how many standard deviations they are away from the average of the past few years. Improving these metrics may be a highly profitable project for utilities in many states to undertake.

## **2.2 Optimization Algorithms Used in Reliability Enhancement**

The focus of this thesis is optimal relay setting and optimal network reconfiguration in power distribution system. The main function of protection on the

power system is to detect and remove the faulted parts as fast and as selectively as possible. The problem of coordinating protective relays in electric power systems consists of selecting their suitable settings such that their fundamental protective function is met under the requirements of sensitivity, selectivity, reliability, and speed. These requirements must be met for a variety of system conditions and configurations, and can be translated into conditions such as: (i) a variety of fault conditions must be detected by the appropriate relays, (ii) the relays located closer to the fault should have priority of operation, (iii) if a primary relay fails, a backup relay should operate, and (iv) the operation of the relay should be as fast as possible to prevent equipment damage, and must occur only in the presence of abnormal operating conditions which jeopardize the system integrity [2]. The devices mostly used for distribution system protection are: breakers and reclosers with different relay functions and fuses.

Directional overcurrent relays are widely used in distribution system. Directional overcurrent relays have two types of settings: time dial setting (*TDS*) and pickup current setting (*I<sub>p</sub>*). In general, the protective relay coordination problem was formulated in previous work either as a linear, nonlinear, or a mixed integer nonlinear programming problem depending on the type of variables in the problem. And the pickup current is the variable that determines the type of the problem according to the relay characteristic functions. When *I<sub>p</sub>* is fixed, the coordination problem becomes a Linear Programming (LP) problem [4-5]. For continuous *I<sub>p</sub>* values, the problem becomes a Nonlinear Programming (NLP) problem, and when discrete values of *I<sub>p</sub>* are taken into account, the problem turns to be a Mixed Integer Nonlinear Programming (MINLP) problem.

In the previous work, due to the complexity of nonlinear optimal programming techniques, the coordination problem was formulated as an LP problem and was solved using LP techniques. These techniques include Simplex, Dual Simplex and Two Phase Simplex. The main disadvantage of this formulation is that the pickup currents and relay characteristic curves are assumed predetermined. Since each relay can allow for various  $I_p$  values and several relay characteristic curves, there could be a better pickup current setting for each relay that would lead to a better objective function.

In this project, I am going to discuss about the digital relays, since both the time dial setting and pickup current setting are continuous, the coordination problem is a Nonlinear Programming (NLP) problem. And for each relay, there will be several options for curve characteristics selection. Hence, the problem becomes a Mixed Integer Nonlinear Programming (MINLP) problem. In addition, coordination of the overcurrent relays and distance relays, and fuse saving scheme will be also considered in the project so that more constraints are put into the optimization problem to make the formulation more complicated and complete. Final optimal relay setting solution is obtained using global solver in GAMS. And in the second half of the thesis, cost-benefit analysis of adding more switches into the system are analyzed.

# **CHAPTER 3**

## **INITIAL RESPONSE**

### **3.1 Introduction**

Associated with the distribution networks themselves are a number of ancillary systems to assist in meeting the requirement for safety, reliability and quality of supply. The most important of these are the protection systems which are installed to clear faults and limit any damage to distribution equipment. Among the principle causes of faults are lightning discharges, the deterioration of insulation, vandalism, and tree branches and animal contacting the electricity circuits. The majority of faults is of a transient nature and can often be cleared with no loss of supply, or just the shortest of interruptions, whereas permanent faults can result in longer outages. In order to avoid damage, suitable and reliable protection should be installed on all circuits and electrical equipment. Protective devices initiate the isolation of faulted sections of the network in order to maintain supplies elsewhere on the system. This then leads to an improved electricity service with better continuity and quality of supply.

A properly coordinated protection system is vital to ensure that an electricity distribution network can operate within preset requirement for safety for individual items of equipment, staff and public, and the network overall. Automatic operation is necessary to isolate faults on the networks as quickly as possible in order to minimize damage. The economic costs and the benefits of a protection device should also be considered to arrive at a suitable balance between the requirements of the scheme and the available financial resources.

The main function of protection on the power system is to detect and remove the faulted parts as fast and as selectively as possible. The problem of coordinating protective relays in electric power systems consists of selecting their suitable settings such that their fundamental protective function is met under the requirements of sensitivity, selectivity, reliability, and speed. These requirements must be met for a variety of system conditions and configurations, and can be translated into conditions such as: (i) a variety of fault conditions must be detected by the appropriate relays, (ii) the relays located closer to the fault should have priority of operation, (iii) if a primary relay fails, a backup relay should operate, and (iv) the operation of the relay should be as fast as possible to prevent equipment damage, and must occur only in the presence of abnormal operating conditions which jeopardize the system integrity[2]. The devices most used for distribution system protection are: over current relays, reclosers and fuses. Their characteristics and coordination between each other will be discussed in the following sections.

### **3.2 Relays**

The evolution of protection relays started with the electromechanical relays and the design of the protection relays has changed significantly over the past years with the advancement in microprocessor and signal processing technology. The first commercial microprocessor based relay was introduced in 1984. Subsequently in the 1990s microprocessor technology, along with the improvements in mathematical algorithms, spurred the development of the so-called numerical relays which are extremely popular for their multifunctional capabilities, low prices and reliability.

Traditional protective relays are usually set offline and kept constant during operation. Settings are normally calculated based on the maximum generation mode in the power system and may not be at optimal performance. In the worst case, when fault occurs under minimum generation, the performance of protection relays will decrease because of the poor sensitivity of the protection relays or even failure of operation may take place. With enlargement of power system, network structure of power supply and distribution line becomes complex and traditional protection of it cannot satisfy the requirement of power system. Appearance of adaptive protection offers an effective method to solve this problem. It can adapt to the changes of different topology and fault types of power system and then change the setting of the relays to an optimal value. Adaptive relay programming are proposed to combat sustained power outages resulting from wind and lightning related weather events, and it is claimed that the SAIDI reliability metric can be improved by as much as 30% annually.

Directional over current relay and distance relay are the most commonly used protective relays in power distribution systems. These two types of relays will be discussed separately in the following sections. And optimization algorithms will be built to find the optimal settings.

### **3.2.1 Adaptive Relay Scheme - Directional Over current relay**

#### **3.2.1.1 Introduction**

The following work is based on the assumption that the potential fault area is determined by the weather information, and relay settings are going to be optimized so that the protection devices in the system can react optimally to the fault.

Directional relays operate only when the fault current flows in the specific tripping direction, they avoid compromising line protection and provide selectivity. Directional over current relays have two types of settings: time dial setting ( $TDS$ ) and pickup current setting ( $I_p$ ). The settings should be chosen to minimize the overall time of operation of relays while maintaining selectivity and reliability. Thus, the directional over current relay coordination problem involves optimization, where the solution is the optimal settings of each relay.

Generally speaking, the over current relay coordination problem was formulated in previous work as a linear, nonlinear or a mixed integer nonlinear programming problem. And the pickup current is the variable that determines the type of the problem according to the relay characteristic functions. When  $I_p$  is fixed, the coordination problem becomes a Linear Programming (LP) problem [4-5]. For continuous  $I_p$  values, the problem becomes a Nonlinear Programming (NLP) problem, and when discrete values of  $I_p$  are taken into account, the problem turns to be a Mixed Integer Nonlinear Programming (MINLP) problem. In this project, we are going to discuss about the digital relays, since both the time dial setting and pickup current setting are continuous, the coordination problem is a Nonlinear Programming (NLP) problem. In addition, for each relay, there will be several options for curve characteristics selection. Hence, the problem becomes a Mixed Integer Nonlinear Programming (MINLP) problem.

#### 3.2.1.2 MINLP Formulation for Optimal Over Current Relay Setting

The relay coordination algorithm is to calculate the time dial setting ( $TDS$ ) and pickup current setting ( $I_p$ ) with the objective of minimizing the primary relay operation

time with backup relay coordinated at all possible fault locations. The objective function can be stated as follows:

$$z = \min \sum_j T_{i,j} \quad \forall j \in L$$

Where

$T_{i,j}$  refers to the operation time of relay  $i$  for a fault at location  $j$

$L$  is a set of possible fault locations

$i$  indicates the nearest relay to the fault,  $i=F(j)$

The objective function is to be achieved under the following constraints:

**A. Coordination criteria**

$$T_{i-1,j} - T_{i,j} \geq \Delta T$$

Where  $T_{i-1,j}$  is the operation time of the upstream relay of relay  $R_i$  for a given fault at place  $j$ .  $\Delta T$  is the coordination time interval between primary relay and backup relay which includes the breaker operating time, relay overrun time after the fault has been cleared and a safety margin to compensate for possible deviations. In numerical relays there is no overrun, and therefore the margin could be chosen as 0.2s [6].

**B. Bounds on relay settings**

$$TDS_{i_{\min}} \leq TDS_i \leq TDS_{i_{\max}} \quad \forall i$$

$$Ip_{i_{\min}} \leq Ip_i \leq Ip_{i_{\max}} \quad \forall i$$

Where  $TDS$  is the time dial setting and  $Ip$  is the pickup current. In most modern relays the time dial settings can start from values as low as 0.1s, and goes to as high as 20s. In distribution systems where it is possible to increase the loading on feeders under

emergency conditions, the minimum pickup current setting is usually 2 times the nominal circuit current. And in order to make sure that the relay is able to trip under fault condition, the maximum pick up current is usually chosen to be half of the smallest single phase to ground fault current. Then the constraints of the relay setting can be rewritten as

$$0.1 \leq TDS_i \leq 20 \quad \forall i$$

$$2I_{norm,i} \leq Ip_i \leq \frac{1}{2} I_{ph-g,i} \quad \forall i$$

### C. Relay characteristics

All relays are assumed identical and with characteristic function approximated by:

$$T_{i,j} = \left( \frac{A_k}{(I_{ij} / Ip_i)^{C_k} - 1} + B_k \right) \times TDS_i$$

Where  $I_{ij}$  is the fault current passing through the relay  $i$  for a fault at place  $j$ , and  $A$ ,  $B$  and  $C$  are constant values to provide selected curve characteristics. It can be seen from the equation that the non-linearity comes from the pickup current term. By adjusting the physical design parameters different time current characteristic can be implemented. The time current characteristics are classified according to the steepness of the curves and the overall time delay as:

- Short time
- Long time
- Definite Minimum Time
- Moderately Inverse
- Inverse

- Very Inverse, and
- Extremely Inverse

According to IEEE Std C37.112-1996, the IEEE Standard Inverse-Time Characteristic Equations for over current relays, the constant and exponents in Table 3.1 define the shape of the standard Moderately Inverse, Very Inverse, and Extremely Inverse trip characteristics.

Table 3.1- Constants and exponents for standard characteristics of overcurrent relays

Characteristic	A	B	C
Moderately Inverse	0.0515	0.1140	0.0200
Very Inverse	19.61	0.491	2.0000
Extremely Inverse	28.2	0.1217	2.0000

As a result, an additional parameter should be added to represent the choice of the time current characteristics curve, whether it is moderately inverse (1), very inverse (2) or extremely inverse (3).

$$K = 1, 2 \text{ or } 3 \quad \forall i$$

In this research area, only these three shapes will be considered. And different  $k$  indicates a different group of  $A$ ,  $B$  and  $C$ . In order to translate this constraint into a mathematical way, the time current characteristics curve selection can be reformulated as follows

$$A = 0.0515 + K_1(19.61 - 0.0515) + K_2(28.2 - 0.0515)$$

$$B = 0.114 + K_1(0.491 - 0.114) + K_2(0.1217 - 0.114)$$

$$C = 0.02 + K_1(2 - 0.02) + K_2(2 - 0.02)$$

Where

$$K_1 + K_2 \leq 1$$

$$K_1, K_2 = 0 \text{ or } 1$$

So that each time only one of the time current characteristics curves is chosen. For example, when  $K_1=0$  and  $K_2=0$ , then  $A=0.0515$ ,  $B=0.114$  and  $C=0.02$ , so moderately inverse is picked. When  $K_1=1$  and  $K_2=0$ , then  $A=19.61$ ,  $B=0.491$  and  $C=2$ , so very inverse is chosen. When  $K_1=0$  and  $K_2=1$ , then  $A=28.2$ ,  $B=0.1217$  and  $C=2$ , which means extremely inverse is chosen. If there are more time current characteristics curves, they can all be written in this way to be formulated into the optimization problem.

In summary, the optimization problem, in term of the relay operation times has the following basic form:

$$z = \min \sum_j T_{i,j} \quad \forall j \in L$$

Subject to:

$$T_{i-1,j} - T_{i,j} \geq \Delta T$$

$$TDS_{i\min} \leq TDS_i \leq TDS_{i\max} \quad \forall i$$

$$Ip_{i\min} \leq Ip_i \leq Ip_{i\max} \quad \forall i$$

$$T_{i,j} = \left( \frac{A_k}{(I_{ij} / Ip_i)^{C_k} - 1} + B_k \right) \times TDS_i$$

Where

$T_{i,j}$  refers to the operation time of relay  $i$  for a fault at location  $j$

$L$  is a set of possible fault locations

$i$  indicates the nearest relay to the fault,  $i=F(j)$

$T_{i-1,j}$  is the operation time of the upstream relay of relay  $i$  for a given fault at place  $j$

$\Delta T$  is the coordination time interval between primary relay and backup relay

$TDS$  is the time dial setting and  $I_p$  is the pickup current

### 3.2.1.3 Case Study

A simple distribution system is built in WinIGS in Fig. 3.1. There is one substation with two feeders. Feeder 3.1 is protected by a breaker at the substation, two reclosers at the indicated location and fuse at the indicated lateral. Feeder 3.2 is connected to feeder 1 with a normally open switch and has one breaker and one recloser along the transmission line. Assume that both the breaker and the recloser are equipped with numerical relays which have over current protection with one of the following selections:

$$\text{Moderately Inverse: } T = \left( \frac{0.0515}{(I_{ij} / I_{p_i})^{0.02} - 1} + 0.114 \right) \times TDS_i$$

$$\text{Very Inverse: } T = \left( \frac{19.61}{(I_{ij} / I_{p_i})^2 - 1} + 0.491 \right) \times TDS_i$$

$$\text{Extremely Inverse: } T = \left( \frac{28.2}{(I_{ij} / I_{p_i})^2 - 1} + 0.1217 \right) \times TDS_i$$

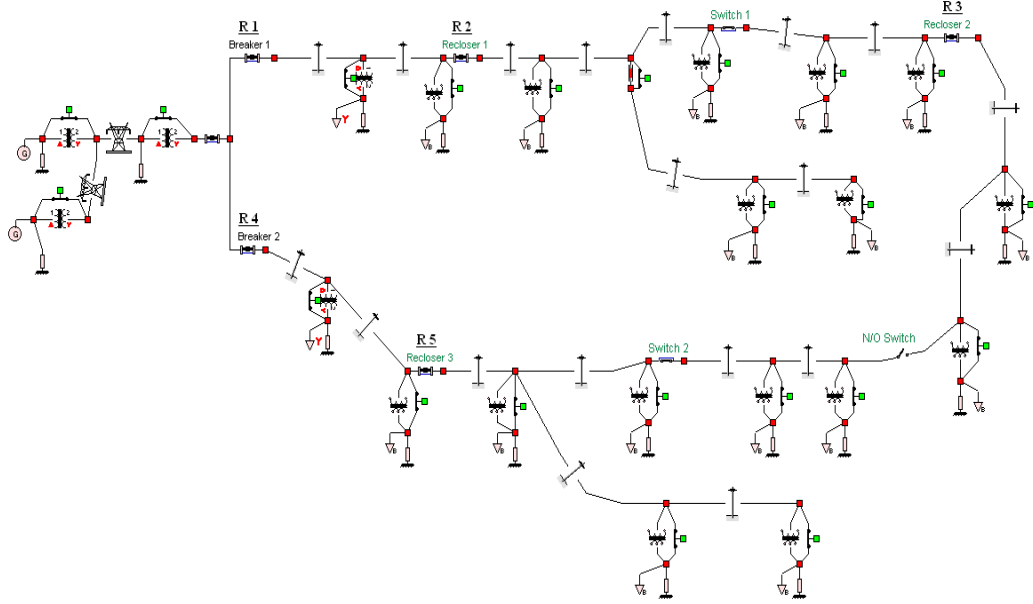


Figure 3.1 Example distribution system

The locations of the breakers and reclosers are shown in Fig. 3.1. According to the requirements and rules for relay settings which are discussed in 1.2.1, the coordination problem can be stated below.

$$z = \min \sum_j T_{i,j}$$

s.t.

(Bounds on relay settings)

$$0.1 \leq TDS_i \leq 20 \quad \text{for } i = 1, 2, 3, 4, 5$$

$$2I_{norm,i} \leq Ip_i \leq \frac{1}{2}I_{ph-g,i} \quad \text{for } i = 1, 2, 3, 4, 5$$

(Coordination criteria)

$$T_{1,j} - T_{2,j} \geq \Delta T$$

$$T_{2,j} - T_{3,j} \geq \Delta T$$

$$T_{4,j} - T_{5,j} \geq \Delta T$$

(Relay characteristics)

$$T_{i,j} = \left( \frac{A_i}{(I_{i,j} / I_{p_i})^{C_i} - 1} + B_i \right) \times TDS_i \quad \text{for } i = 1, 2, 3, 4, 5$$

Where

$$A_i = 0.0515 + K_{i,1}(19.61 - 0.0515) + K_{i,2}(28.2 - 0.0515)$$

$$B_i = 0.114 + K_{i,1}(0.491 - 0.114) + K_{i,2}(0.1217 - 0.114)$$

$$C_i = 0.02 + K_{i,1}(2 - 0.02) + K_{i,2}(2 - 0.02)$$

$$K_{i,1} + K_{i,2} \leq 1$$

$$K_{i,1}, K_{i,2} = 0 \text{ or } 1$$

The algorithm is implemented to solve the relay optimization problem in Fig. 3.1. Assume the coordination time between the upstream and downstream relay is 0.2s as is discussed in section 3.1.2.1. The lower bond and upper bond of the pickup current of each relay can be read from the simulation result of WinIGS and is listed in Table 3.2. After simulating faults at all the possible locations 1, 2, 3, 4 and 5, as is shown in Fig3.2, fault current at each relay are recorded in Table 3.3.

Table 3.2 - Constraints of the pickup current of each relay

Relay	Lower bound	Upper bound
1	340	375
2	180	355
3	60	350
4	320	395
5	160	380

Table 3.3 – Fault current at each relay to different fault locations

	Location 1	Location 2	Location 3	Location 4	Location 5
Fault Current at R1	1875	870	752		
Fault Current at R2		837	714		
Fault Current at R3			685		
Fault Current at R4				1444	790
Fault Current at R5					760

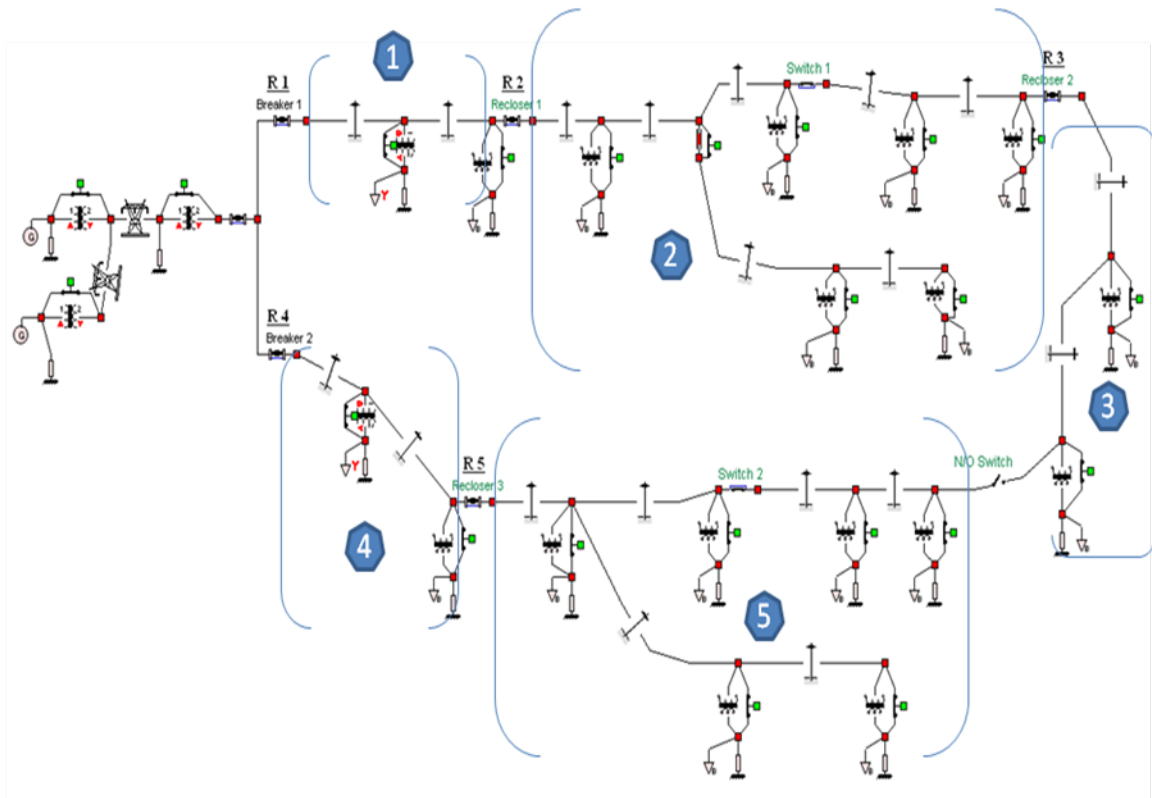


Figure 3.2 Fault simulation in the example distribution system

The detailed equations of the problem are as follows:

$$\min T_{1,1} + T_{2,2} + T_{3,3} + T_{4,4} + T_{5,5}$$

*s.t.*

(Bounds on relay settings)

$$0.1 \leq TDS_i \leq 20 \quad i=1, 2, 3, 4 \text{ and } 5$$

$$340 \leq Ip_1 \leq 375$$

$$180 \leq Ip_2 \leq 355$$

$$60 \leq Ip_3 \leq 350$$

$$320 \leq Ip_4 \leq 395$$

$$160 \leq Ip_5 \leq 380$$

(Case 1: When fault occurs at place 1)

$$T_{1,1} = \left( \frac{A_{k_1}}{(I_{1,1} / Ip_1)^{C_{k_1}} - 1} + B_{k_1} \right) \times TDS_1$$

(Case2: When fault occurs at place 2)

$$T_{1,2} = \left( \frac{A_{k_1}}{(I_{1,2} / Ip_1)^{C_{k_1}} - 1} + B_{k_1} \right) \times TDS_1$$

$$T_{2,2} = \left( \frac{A_{k_2}}{(I_{2,2} / Ip_2)^{C_{k_2}} - 1} + B_{k_2} \right) \times TDS_2$$

$$T_{1,2} - T_{2,2} \geq 0.2$$

(Case 3: When fault occurs at place 3)

$$T_{1,3} = \left( \frac{A_{k_1}}{(I_{1,3} / Ip_1)^{C_{k_1}} - 1} + B_{k_1} \right) \times TDS_1$$

$$T_{2,3} = \left( \frac{A_{k_2}}{(I_{2,3} / Ip_2)^{C_{k_2}} - 1} + B_{k_2} \right) \times TDS_2$$

$$T_{3,3} = \left( \frac{A_{k_3}}{(I_{3,3} / Ip_2)^{C_{k_3}} - 1} + B_{k_3} \right) \times TDS_3$$

$$T_{1,3} - T_{2,3} \geq 0.2$$

$$T_{2,3} - T_{3,3} \geq 0.2$$

(Case 4: When fault occurs at place 4)

$$T_{4,4} = \left( \frac{A_{k_4}}{(I_{4,4} / Ip_4)^{C_{k_4}} - 1} + B_{k_4} \right) \times TDS_4$$

Case 5: When fault occurs at place 5

$$T_{4,5} = \left( \frac{A_{k_4}}{(I_{4,5} / Ip_4)^{C_{k_4}} - 1} + B_{k_4} \right) \times TDS_4$$

$$T_{5,5} = \left( \frac{A_{k_5}}{(I_{5,5} / Ip_5)^{C_{k_5}} - 1} + B_{k_5} \right) \times TDS_5$$

$$T_{4,5} - T_{5,5} \geq 0.2$$

(Relay time current characteristic curve selection constraints)

$$A_i = 0.0515 + K_{i,1} \times (19.61 - 0.0515) + K_{i,2} \times (28.2 - 0.0515) \quad \text{for } i = 1, 2, 3, 4 \text{ and } 5$$

$$B_i = 0.114 + K_{i,1} \times (0.491 - 0.114) + K_{i,2} \times (0.1217 - 0.114) \quad \text{for } i = 1, 2, 3, 4 \text{ and } 5$$

$$C_i = 0.02 + K_{i,1} \times (2.0 - 0.02) + K_{i,2} \times (2.0 - 0.02) \quad \text{for } i = 1, 2, 3, 4 \text{ and } 5$$

$$K_{i,1} + K_{i,2} \leq 1 \quad \text{for } i = 1, 2, 3, 4 \text{ and } 5$$

$$K_{i,1}, K_{i,2} = 0 \text{ or } 1$$

The optimization problem is built in LINGO. Using MINLP function, the result is shown in Table 3.4. The codes for the programming and the results from LINGO are in Appendix C. In order to demonstrate the effectiveness of the proposed algorithm, the widely used LP is also tested in the same distribution system. In the LP formulation, the objective function and the coordination criteria are the same as the ones in MINLP formulation. The differences come from the constraints of pickup current and the selection of relay functions. In LP formulation, the pickup up current and time current characteristic curve of each relay are determined by experience, and only the *TDS* is optimized. The formulation is listed below. And by using LP function in LINGO, the result is also shown in Table 3.4.

$$z = \min \sum_j T_{i,j}$$

s.t.

(Bounds on relay settings)

$$0.1 \leq TDS_i \leq 20 \quad \text{for } i = 1, 2, 3, 4, 5$$

(Coordination criteria)

$$T_{1,j} - T_{2,j} \geq \Delta T$$

$$T_{2,j} - T_{3,j} \geq \Delta T$$

$$T_{4,j} - T_{5,j} \geq \Delta T$$

(Relay characteristics)

$$T_{i,j} = \left( \frac{A_i}{(I_{i,j} / I_{p_i})^{C_i} - 1} + B_i \right) \times TDS_i \quad \text{for } i = 1, 2, 3, 4, 5$$

Where

$A_i, B_i, C_i$  and  $I_{p_i}$  are determined

Table 3.4 – Results for the MINLP and LP formulation

	Relay	TDS	Pickup Current	TC curve	Objective Value
MINLP	Relay 1	0.112	375	Extremely Inverse	0.4248
	Relay 2	0.1	201	Extremely Inverse	
	Relay 3	0.1	60	Very Inverse	
	Relay 4	0.1	331.1	Extremely Inverse	
	Relay 5	0.1	160	Extremely Inverse	
LP	Relay 1	0.178	360	Extremely Inverse	0.9052
	Relay 2	0.1	300	Extremely Inverse	
	Relay 3	0.1	200	Extremely Inverse	
	Relay 4	0.126	370	Extremely Inverse	
	Relay 5	0.1	250	Extremely Inverse	

Compare the results from MINLP and LP formulation of the optimal relay setting, it can be seen clearly from the table that MINLP can realize relay operation much faster than LP by optimizing the relay settings.

### 3.2.2 Adaptive Relay Scheme - Distance Relay

Distance relay are set on the basis of the positive sequence impedance from the relay location up to the point on the line to be protected. Line impedances are proportional to the line lengths and it is this property that is used to determine the position of the fault, starting from the location of the relay.

Normally, three protection zones in the direction of the fault are used in order to cover a section of line and to provide back-up protection to remote sections. In the majority of cases the setting of the reach of the three main protection zones is made in accordance with the following criteria [6] (as is shown in Figure 3.3):

Zone 1: this is set to cover between 80 and 85 per cent of the length of the protected line;

Zone 2: this is set to cover all the protected line plus 50 per cent of the shortest next line;

Zone 3: this is set to cover all the protected line plus 100 per cent of the second longest line, plus 25 per cent of the shortest next line.

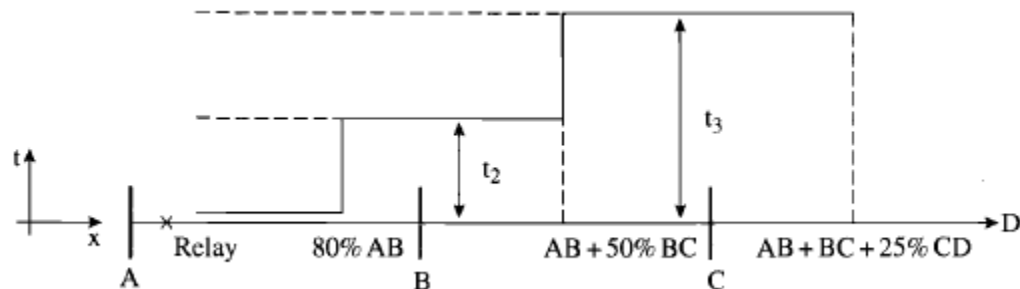


Figure 3.3 Distance relay protection zone for a radial system

In addition to the unit for setting the reach, each zone unit has a timer unit. The operating time for zone 1,  $t_1$ , is normally set by the manufacturer to trip instantaneously since any fault on the protected line detected by the zone 1 unit should be cleared immediately without the need to wait for any other device to operate. This operation is fast with just a small delay (two to three cycles) to avoid tripping on transients. The

operating time for zone 2 is usually of the order of 0.25 to 0.4 s, and that of zone 3 is in the range of 0.6 to 1.0 s.

Since the tripping produced by zone 1 is instantaneous, it should not reach as far as the bus at the end of the first line so it is set to cover only 80-85% of the protected line. The remaining 20-15% provides a factor of safety in order to mitigate against errors introduced by the measurement transformers and line impedance calculations. The 20-15% to the end of the line is protected by zone 2, which operates in  $t_2$  s. Zone 3 provides the back-up and operates with a delay of  $t_3$  s. Since the reach and therefore the operating time of the distance relays are fixed, their co-ordination is much easier than that for overcurrent relays.

### **3.2.3 Coordination of over current relays and distance relays**

It has been shown that when the line protection schemes are composed of distance relays and overcurrent relays, the setting of the relays must be computed considering both relays. Separate relay computation would lead to loss of selectivity. Thus, it is useful to include distance relays parameters in the process of computing the time dial settings of over current relays in distribution system which have a mixed scheme with overcurrent relays and distance relays.

#### **3.2.3.1 Formulation for coordination of overcurrent and distance relay**

The problem of finding the time dial setting of directional overcurrent relays has been stated and solved in section 3.2.1 using Mixed Integer Linear Programming technique. The technique is based on the mathematical statement of the sensitivity, speed

and selectivity conditions associated with the relay coordination problem. The basic optimization problem, in term of the relay operation times has the following basic form:

$$z = \min \sum_j T_{i,j} \quad \forall j \in L$$

Subject to:

$$T_{i-1,j} - T_{i,j} \geq \Delta T$$

$$TDS_{i\min} \leq TDS_i \leq TDS_{i\max} \quad \forall i$$

$$Ip_{i\min} \leq Ip_i \leq Ip_{i\max} \quad \forall i$$

$$T_{i,j} = \left( \frac{A_k}{(I_{ij} / Ip_i)^{C_k} - 1} + B_k \right) \times TDS_i$$

Where

$T_{i,j}$  refers to the operation time of relay  $i$  for a fault at location  $j$

$L$  is a set of possible fault locations

$i$  indicates the nearest relay to the fault,  $i=F(j)$

$T_{i-1,j}$  is the operation time of the upstream relay of relay  $i$  for a given fault at place  $j$

$\Delta T$  is the coordination time interval between primary relay and backup relay

$TDS$  is the time dial setting and  $Ip$  is the pickup current

Figure 3.4 shows the case of two overcurrent relays with similar time current characteristic, where the relevant faults are determined by points F1 and F2[7].

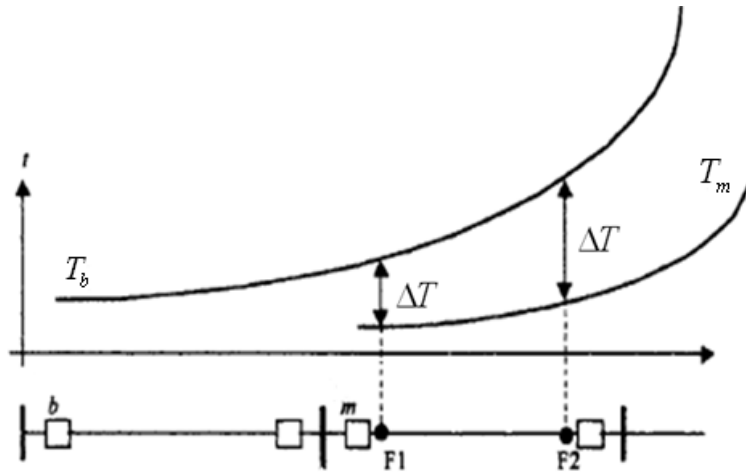


Fig. 3.4 Coordination of overcurrent relays

The derivation of the coordination constraints for system with overcurrent relays and distance relays is explained in Figure 3.5. Second zone of distance relay associated with circuit breaker b must be slower than the overcurrent relays associated with main circuit breaker m, which can be stated as follows:

$$T_{Z_{b,F4}} - T_{m,F4} \geq \Delta T'$$

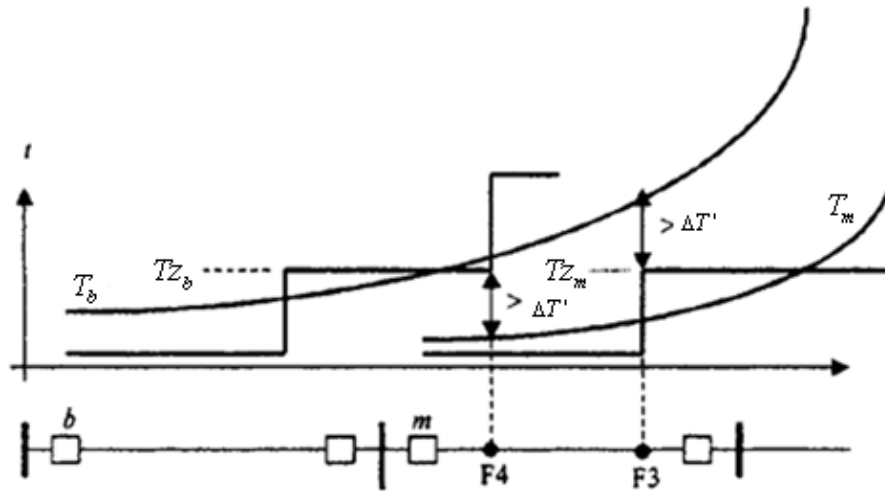


Fig. 3.5 Coordination of overcurrent relays and distance relays

Where  $\Delta T'$  is a time coordination interval used in the selectivity constraints between overcurrent relays and distance relays. For this constraint, the operation time of

main overcurrent relay is evaluated at point F4, which corresponds to the ohmic reach of the second zone of the distance relay associated with the backup circuit breaker. Overcurrent relay associated with circuit breaker b must be slower than the second zone of distance relay associated with main circuit breaker m:

$$T_{b,F3} - T_{z_m,F3} \geq \Delta T'$$

### 3.2.3.2 Case study for coordination of overcurrent and distance relay

All the relays are assumed to have multi functions including the overcurrent relay function and distance relay function. The same example distribution system is used for the optimal relay setting for overcurrent relays and distance relays. Eight faults, as is shown in Figure 3.6, are simulated in the test system. Short circuit currents for the faults are calculated and recorded in Table 3.5.

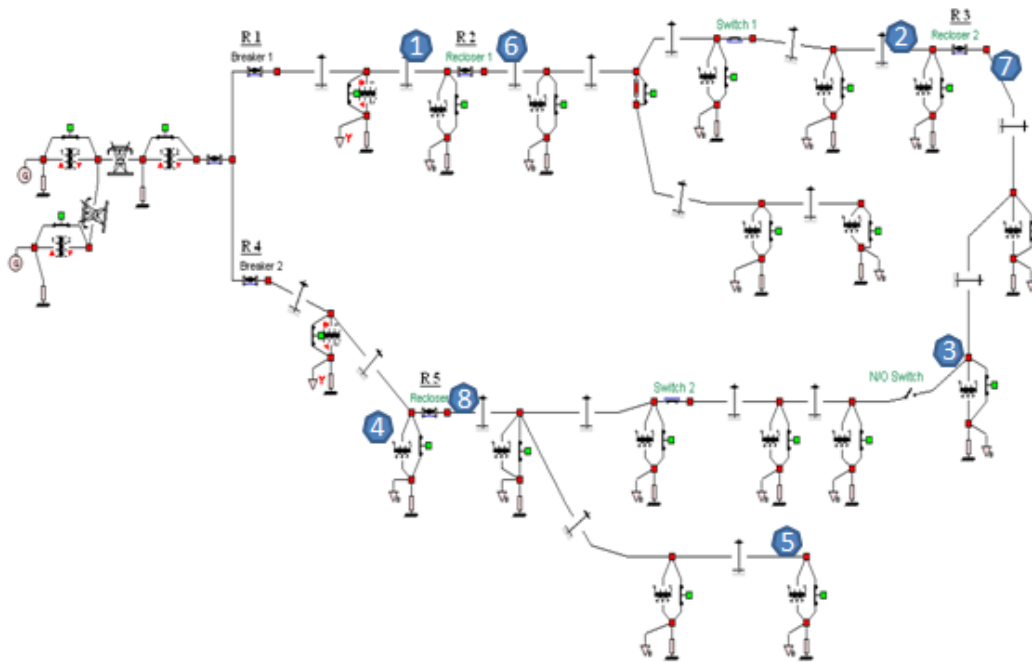


Fig. 3.6 Test system for coordination of overcurrent relay and distance relay

Table 3.5 – Fault current at each relay to 8 different fault locations

	Fault Current(A) /impedance(Ω) at R1	Fault Current(A) /impedance(Ω) at R2	Fault Current(A) /impedance(Ω) at R3	Fault Current(A) /impedance(Ω) at R4	Fault Current(A) /impedance(Ω) at R5
Location 1	1875				
Location 2	870/9.16	837/8.19			
Location 3	752/10.56	714/7.69	685/3.86		
Location 4				1444	
Location 5				790/9.64	760/6.99
Location 6		1798			
Location 7			799		
Location 8					1380

The detailed equations of the problem are as follows:

$$\min T_{1,1} + T_{2,2} + T_{3,3} + T_{4,4} + T_{5,5} + T_{2,6} + T_{3,7} + T_{5,8}$$

*Subject to*

(Bounds on relay settings)

$$0.1 \leq TDS_i \leq 20 \quad i=1, 2, 3, 4 \text{ and } 5$$

$$0.2 \leq Tz_i \leq 0.6 \quad i=1, 2, 3, 4 \text{ and } 5$$

$$340 \leq Ip_1 \leq 375$$

$$180 \leq Ip_2 \leq 355$$

$$60 \leq Ip_3 \leq 350$$

$$320 \leq Ip_4 \leq 395$$

$$160 \leq Ip_5 \leq 380$$

(Case 1: When fault occurs at place 1)

$$T_{1,1} = \left( \frac{A_{k_1}}{(I_{1,1} / Ip_1)^{C_{k_1}} - 1} + B_{k_1} \right) \times TDS_1$$

(Case2: When fault occurs at place 2)

$$T_{1,2} = \left( \frac{A_{k_1}}{(I_{1,2} / Ip_1)^{C_{k_1}} - 1} + B_{k_1} \right) \times TDS_1$$

$$T_{2,2} = \left( \frac{A_{k_2}}{(I_{2,2} / Ip_2)^{C_{k_2}} - 1} + B_{k_2} \right) \times TDS_2$$

$$T_{1,2} - T_{2,2} \geq 0.2$$

$$T_{1,2} - T_{z_{2,2}} \geq 0.3$$

(Case 3: When fault occurs at place 3)

$$T_{1,3} = \left( \frac{A_{k_1}}{(I_{1,3} / Ip_1)^{C_{k_1}} - 1} + B_{k_1} \right) \times TDS_1$$

$$T_{2,3} = \left( \frac{A_{k_2}}{(I_{2,3} / Ip_2)^{C_{k_2}} - 1} + B_{k_2} \right) \times TDS_2$$

$$T_{3,3} = \left( \frac{A_{k_3}}{(I_{3,3} / Ip_2)^{C_{k_3}} - 1} + B_{k_3} \right) \times TDS_3$$

$$T_{1,3} - T_{2,3} \geq 0.2$$

$$T_{2,3} - T_{3,3} \geq 0.2$$

$$T_{2,3} - T_{z_{3,3}} \geq 0.3$$

(Case 4: When fault occurs at place 4)

$$T_{4,4} = \left( \frac{A_{k_4}}{(I_{4,4} / Ip_4)^{C_{k_4}} - 1} + B_{k_4} \right) \times TDS_4$$

(Case 5: When fault occurs at place 5)

$$T_{4,5} = \left( \frac{A_{k_4}}{(I_{4,5} / Ip_4)^{C_{k_4}} - 1} + B_{k_4} \right) \times TDS_4$$

$$T_{5,5} = \left( \frac{A_{k_5}}{(I_{5,5} / Ip_5)^{C_{k_5}} - 1} + B_{k_5} \right) \times TDS_5$$

$$T_{4,5} - T_{5,5} \geq 0.2$$

$$T_{4,5} - Tz_{5,5} \geq 0.3$$

(Case 6: When fault occurs at place 6)

$$T_{2,6} = \left( \frac{A_{k_2}}{(I_{2,6} / Ip_2)^{C_{k_2}} - 1} + B_{k_2} \right) \times TDS_2$$

$$Tz_{1,6} - T_{2,6} \geq 0.3$$

(Case 7: When fault occurs at place 7)

$$T_{3,7} = \left( \frac{A_{k_3}}{(I_{3,7} / Ip_3)^{C_{k_3}} - 1} + B_{k_3} \right) \times TDS_3$$

$$Tz_{2,7} - T_{3,7} \geq 0.3$$

(Case 8: When fault occurs at place 8)

$$T_{5,8} = \left( \frac{A_{k_5}}{(I_{4,8} / Ip_4)^{C_{k_5}} - 1} + B_{k_5} \right) \times TDS_5$$

$$Tz_{4,8} - T_{5,8} \geq 0.3$$

(Relay time current characteristic curve selection constraints)

$$A_i = 0.0515 + K_{i,1} \times (19.61 - 0.0515) + K_{i,2} \times (28.2 - 0.0515) \quad \text{for } i = 1, 2, 3, 4 \text{ and } 5$$

$$B_i = 0.114 + K_{i,1} \times (0.491 - 0.114) + K_{i,2} \times (0.1217 - 0.114) \quad \text{for } i = 1, 2, 3, 4 \text{ and } 5$$

$$C_i = 0.02 + K_{i,1} \times (2.0 - 0.02) + K_{i,2} \times (2.0 - 0.02) \quad \text{for } i = 1, 2, 3, 4 \text{ and } 5$$

$$K_{i,1} + K_{i,2} \leq 1 \quad \text{for } i = 1, 2, 3, 4 \text{ and } 5$$

$$K_{i,1}, K_{i,2} = 0 \text{ or } 1$$

## Results

The optimization problem is built in LINGO. Using MINLP function, the result is shown in Table 3.6. In paper [7], the researchers used the same second zone time setting for all the distance relays in the system. In this project, second zone time setting of each distance relay is optimized separately. And after comparing the results of case 1 and case 2, it shows that with different second zone timing for each relay, the result is better than the one using one second zone time setting for all the relays. The operation time of relays can save up to 20.73%.

Table 3.6 – Results for the coordination of overcurrent and distance relay setting

	Relay	TDS	Pickup Current	TC curve	2 <sup>nd</sup> zone timing	Objective Value
Case1	Relay 1	0.251	375	Extremely Inverse	0.388	0.9024
	Relay 2	0.1	291.1	Extremely Inverse	0.323	
	Relay 3	0.1	60	Very Inverse	0.2	
	Relay 4	0.126	395	Extremely Inverse	0.351	
	Relay 5	0.1	160	Extremely Inverse	0.2	

Table 3.6 continued

Case 2	Relay 1	0.289	375	Extremely Inverse	0.42	1.1384
	Relay 2	0.1	338.8	Extremely Inverse	0.42	
	Relay 3	0.1	60	Very Inverse	0.42	
	Relay 4	0.181	395	Extremely Inverse	0.42	
	Relay 5	0.1	160	Extremely Inverse	0.42	

### 3.3 Fuse

Fuses act as both a protective and a disconnecting device, and are the earliest and simplest overcurrent protection device in the power system. They basically consist of metallic elements which melt in a time depending on the level of electric current when the current exceeds a certain value. The size and construction of the element is determined so that the heat produced for a normal current does not cause the element to operate. During normal load conditions, the fuse must carry the normal operating current without nuisance openings. However, when an overcurrent occurs the fuse must interrupt the overcurrent and withstand the voltage across the fuse after internal arcing.

Fuse possesses one important advantage over mechanical interrupting devices such as circuit breakers. It operates so quickly that it limits the possible damage to cable and other equipment. The larger the current, the quicker the element melts. More precisely, fuse has the ability to interrupt very large currents in a much shorter time – so short that the current will be ‘cut off’ before it reaches its peak value, which is less than 5

ms in a 50Hz system. On the other hand, replacing a fuse is inconvenient, because it takes longer to replace a fuse than to reclose a circuit breaker.

### **3.3.1 Characteristic Parameters**

#### **Rated Current $I_N$**

$I_N$  is the maximum current that the fuse can continuously conduct without interrupting the circuit. The current rating of a fuse identifies its current carrying capacity based on a controlled set of test conditions.

#### **Rated Voltage $V_N$**

Voltage rating of the fuse must be greater than or equal to what would become the open circuit voltage. Rated voltage should be larger than the maximum voltage source it would have to disconnect.

#### **Temperature**

All electrical characteristics of a fuse are rated and validated at an ambient temperature of 25°C. Both higher and lower ambient temperatures will affect the fuse's opening and current carrying characteristics.

#### **Melting Integral**

$\int i^2 dt$  is called the Joule integral and is usually abbreviated to  $I^2t$  [1]. It is a most convenient way of estimating the heating effect on the fuse due to the overcurrent.

#### **Time Current Curve (TCC)**

The time current characteristic curves of a protective device describe how fast the device responds to the overcurrent condition. Time current characteristics are used in coordinating multiple fuses and other protective equipment installed on the same distribution feeder. Figure 3.7 shows the minimum melting time of a certain class of fuses versus the fault current through the fuse. Similar curves provide the maximum melting time of a fuse versus fault current through the fuse.

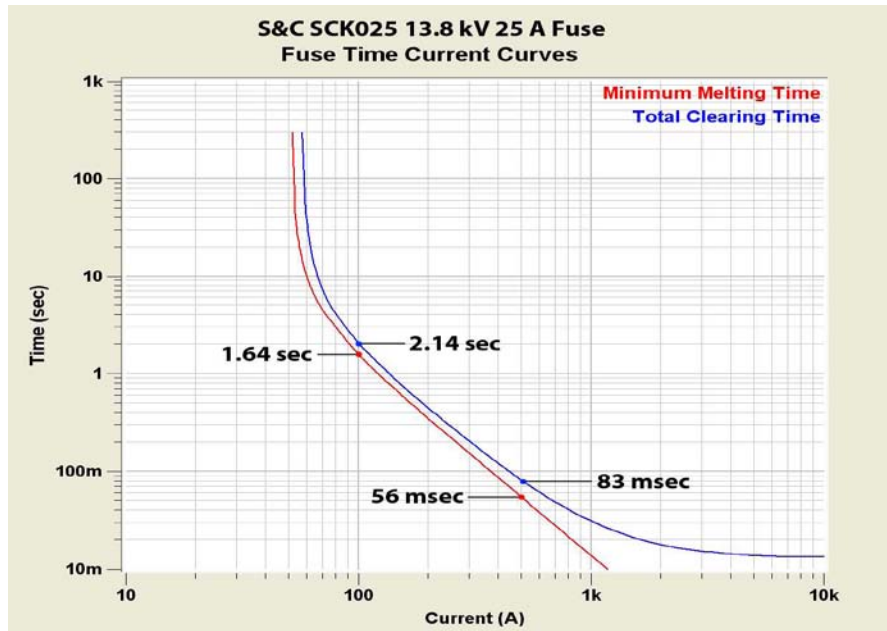


Figure 3.7 Minimum Melting Time and Total Clearing Time for a Specific Fuse [3]

### Melting time

From the figure, we see the time required by a fuse to melt during a fault has a distribution. The difference between the minimum and maximum times can be substantial. Figure 3.3 shows a typical distribution between minimum and maximum melting times. It is easy to understand the distribution in melting times if one considers the following two facts: (a) the initial temperature of the fuse and its housing will vary and it will affect the time at which the filament will reach the melting temperature, and (b) the size (cross

section) of the filament is not constant because of manufacturing imperfections and therefore the thinner parts will reach melting temperature faster than the other parts. Once the filament of the fuse melts, an electric arc is generated in the location of the filament. The housing of the fuse element is designed to quench this electric arc. Various designs are available for this purpose. Once the electric arc has been extinguished, then the fault has been cleared. The time between the initiation of the fault and the extinguishing of the electric arc is the total clearing time of the fuse [3]. The variability of the total clearing time must be considered when fuses are coordinated with other protection devices.

### 3.3.2 Fuse Operation

In the project, the magnitude of the fault current will be provided for each particular fuse at different locations. Given the fuse size and manufacture data, the time current curve of the fuse is known. Our Objective is to determine whether and when the fuse will melt.

A trial and error method is developed to achieve this objective using the following procedure.

1. Given the fault time-current curve, initiate fuse starting melting time  $t_1$ , as is shown in figure 3.8
2. Use time current curve for the particular fuse,  $t_1 = f_{\min}(I_1)$ , calculate the value of  $I_1$ , as is shown in figure 3.9
3. Compare the joule energy of  $\int_0^{t_1} i_{fault} dt$  and  $I_1^2 t_1$

If the former is bigger than the latter, decrease  $t_1$ , and then go to step 2

If the former is smaller than the latter, increase  $t_1$ , and then go to step 2

4. When  $\int_0^{t_1} i_{fault} dt$  equals  $I_1^2 t_1$ , then  $t_1$  is the starting melting time of the fuse

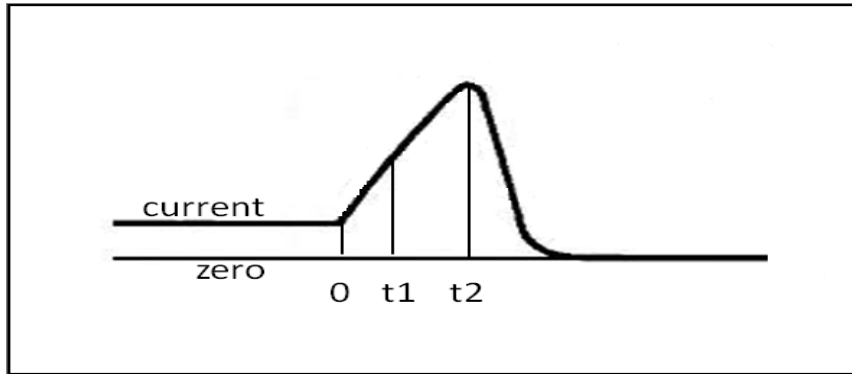


Figure 3.8 Fault time current curve

Total clearing time calculation follows the same step as the calculation of starting melting time.

1. Initiate total clearing time  $t_2$ , and  $t_2 > t_1$ , as is shown in figure 3.8
2. Use time current curve for the particular fuse,  $t_2 = f_{max}(I_2)$ , calculate the value of  $I_2$ , as is shown in figure 3.9

3. Compare the joule energy of  $\int_0^{t_2} i_{fault} dt$  and  $I_2^2 t_2$

3.1 If the former is bigger than the latter, decrease  $t_2$ , and then go to step 2

3.2 If the former is smaller than the latter, increase  $t_2$ , and then go to step 2

4. When  $\int_0^{t_2} i_{fault} dt$  equals  $I_2^2 t_2$ , then  $t_2$  is the starting melting time of the fuse, and

$\Delta t = t_2 - t_1$  is the fuse melting time

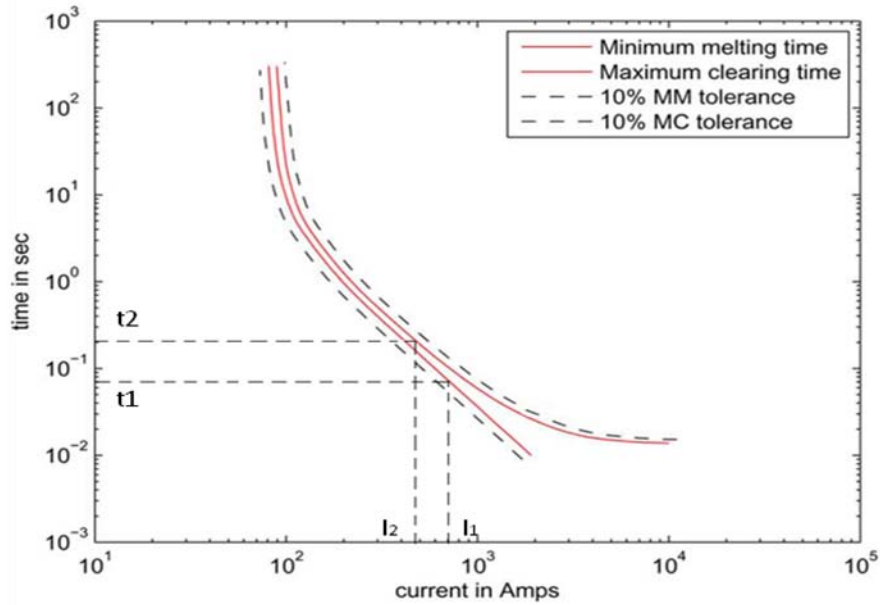


Figure 3.9 Time current curve for fuse 40K

### 3.4 Coordination of Relays and Fuses

Fuse blow and fuse saving scheme are widely used in distribution system. For fuse blow scheme, breaker is slow to trip so that fuse is allowed to blow for most faults, as is shown in Figure 3.10. It is used primarily to minimize momentary interruptions (reduce MAIFI) and is useful in high short circuit current areas and more suitable for industrial type customers having high sensitive loads. For fuse saving scheme, breaker is tripping on fast or instantaneous pickup to clear temporary fault without blowing fuse, as is shown in Figure 3.11. It is used to minimize customer interruption time, and it can reduce SAIDI but at the same time increase MAIFI. Fuse saving scheme works well in most areas especially for residential and small commercial customers, however, not suitable for certain industrial customers that cannot tolerate immediate reclosing.

Many utilities use both schemes for a variety of reasons. They use fuse saving on overhead and fuse blow on underground taps; they use fuse saving on rural and fuse blow in urban; they use fuse save on stormy days and fuse blow on nice days; they use fuse saving on some circuits and fuse blow on others depending on customer desires.

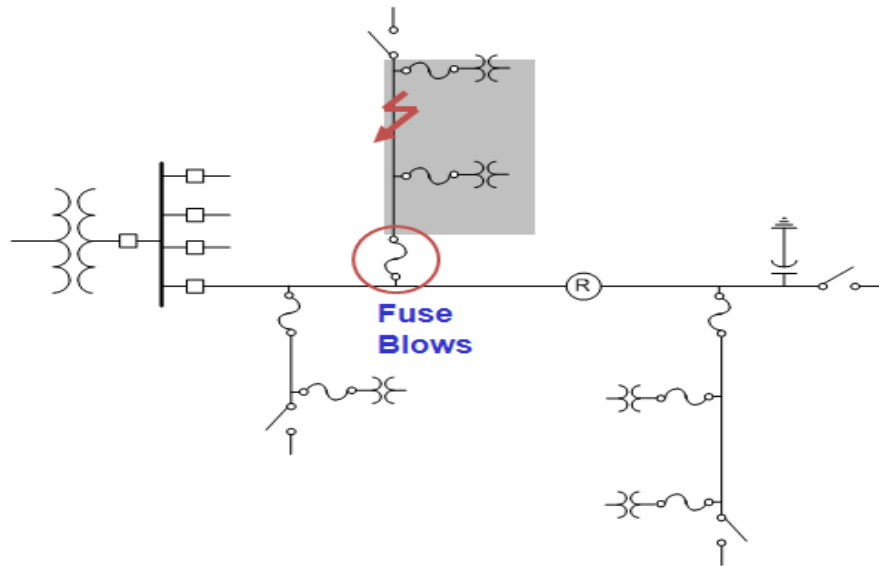


Figure 3.10 Fuse blow scheme

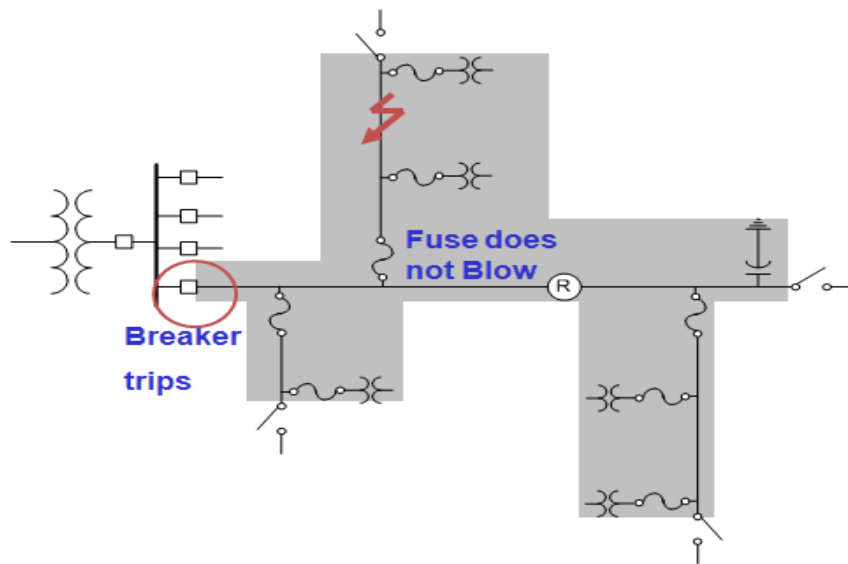


Figure 3.11 Fuse saving scheme

In this project, the research is emphasized on the improvement of SAIDI in bad weather conditions. So fuse saving scheme is recommended as most of the faults occurred in severe weather conditions are momentary which are caused by lightning, wind, tree branches and so on.

Take the test system in Figure 3.6 as an example, recloser 2 should operate faster than the fuse in lateral to prevent the fuse from blowing. After putting the constraints into the optimal relay setting algorithm, the new settings of the relays in the system will be generated. A more detailed example is listed in the next section.

### **3.5 Test System**

This section provides an overview of the adaptive relay programming approach used for optimal relay setting for an example test system of IEEE 123 Node Test Feeder.

#### **3.5.1 System Description**

Figure 3.12 shows the original IEEE 123 node test system. The IEEE 123 node test feeder operates at a nominal voltage of 13.8 kV. There are enough switches in the feeder so that optimal configuration procedures can be tested. This is the most comprehensive feeder and is characterized by:

1. Overhead and underground line segments with various phasing.
2. Unbalanced loading with all combinations of load types (PQ, constant I, constant Z)
3. All loads are “spot loads” located at a node
4. Four step-type voltage regulators

- 5. Shunt capacitor banks
- 6. Switching to provide alternate paths of power-flow

This feeder is well behaved and does not have a convergence problem. It provides a test of the modeling of the phasing of the lines. The four voltage regulators provide a good test to assure that the changing of individual regulator taps is coordinated with the other regulators. A complete description of the ratings of all the equipment in the system is given in Appendix B.

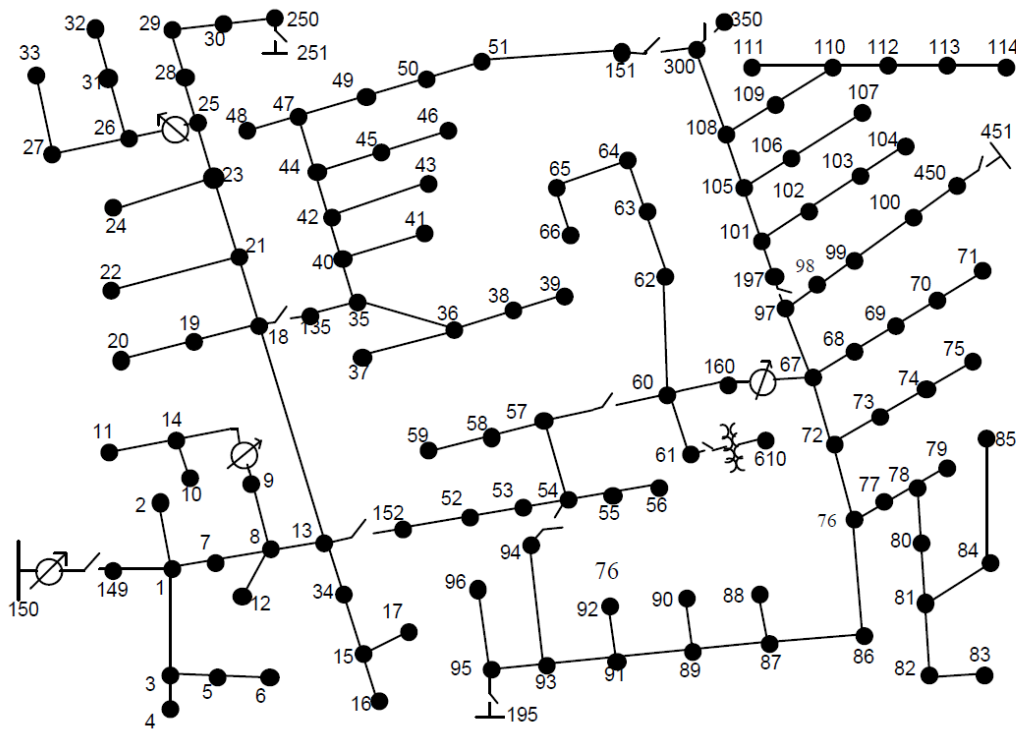


Figure 3.12 IEEE 123-Node Test Feeder

Figure 3.13 is the same test system built in WinIGS – F for simulation and computation. Fuses and relays are added to the original system for the purpose of optimal relay programming.

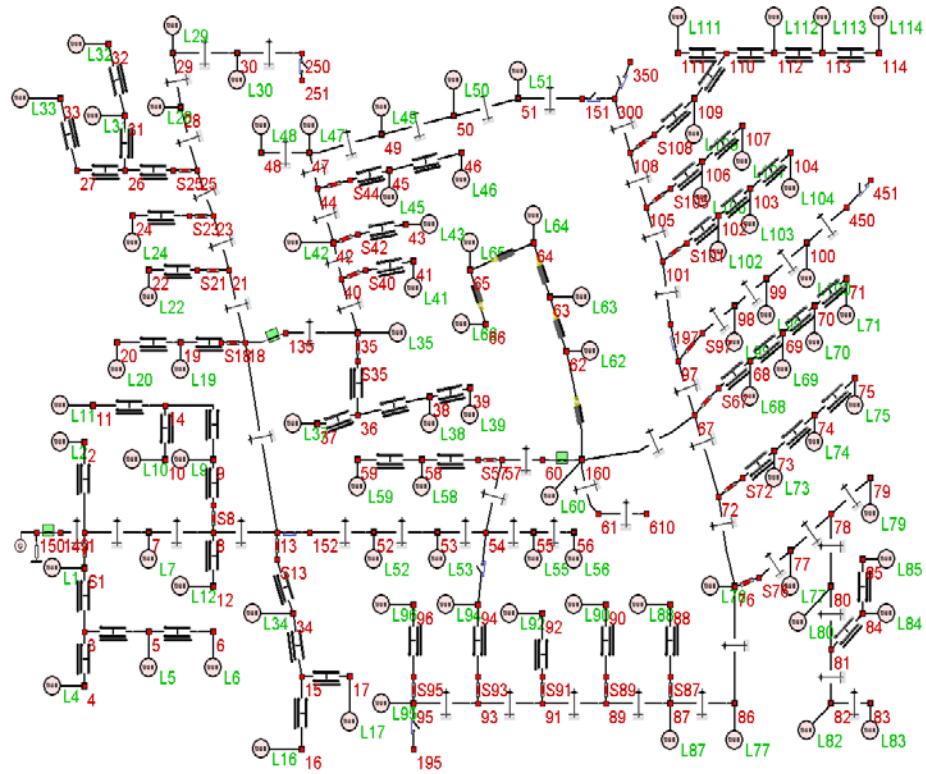


Figure 3.13 IEEE 123-Node Test Feeder in WinIGS - F

### 3.5.2 Problem Formulation

The lower bond and upper bond of the pickup current of each relay can be read from the simulation result of WinIGS – F, and is listed in Table 3.7. After simulating faults at all the possible locations, as is shown in Figure 3.14, fault current at each relay is recorded in Table3.8.

Table 3.7 Constraints of the pickup current in IEEE 123 node test system

Relay	Lower Bond	Upper Bond
1	300	500
2	100	400
3	150	300

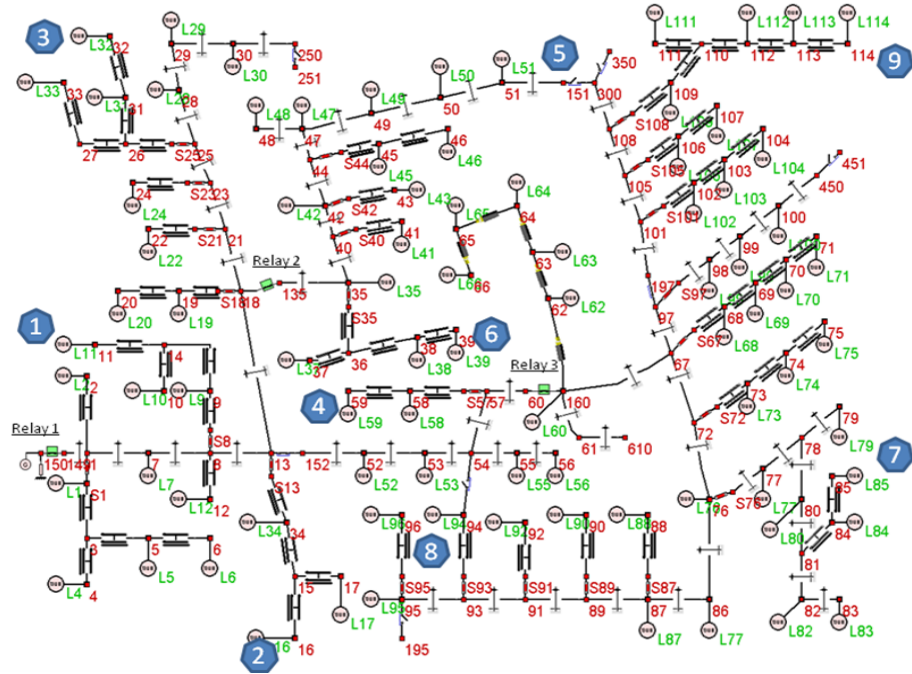


Figure 3.14 IEEE 123-Node Test Feeder with fault simulation

Table 3.8 Fault current in IEEE 123 node test system

Location	Fault Current at R1	Fault Current at R2	Fault Current at R3	Fault Current at Fuse
1	1002			945
2	1016			980
3	685			630
4	726			700
5	583	522		
6	662	626		618
7	422		381	362
8	454		400	380
9	432		372	352

The detailed equations of the problem are as follows:

$$\min T_{1,1} + T_{1,2} + T_{1,3} + T_{1,4} + T_{2,5} + T_{2,6} + T_{3,7} + T_{3,8} + T_{3,9}$$

Subject to

(Bounds on relay settings)

$$0.1 \leq TDS_i \leq 20 \quad i=1, 2 \text{ and } 3$$

$$300 \leq Ip_1 \leq 400$$

$$60 \leq Ip_2 \leq 300$$

$$120 \leq Ip_3 \leq 200$$

(Case 1: When fault occurs at place 1)

$$T_{1,1} = \left( \frac{A_{k_1}}{(I_{1,1} / Ip_1)^{C_{k_1}} - 1} + B_{k_1} \right) \times TDS_1$$

(Case2: When fault occurs at place 2)

$$T_{1,2} = \left( \frac{A_{k_1}}{(I_{1,2} / Ip_1)^{C_{k_1}} - 1} + B_{k_1} \right) \times TDS_1$$

(Case 3: When fault occurs at place 3)

$$T_{1,3} = \left( \frac{A_{k_1}}{(I_{1,3} / Ip_1)^{C_{k_1}} - 1} + B_{k_1} \right) \times TDS_1$$

(Case 4: When fault occurs at place 4)

$$T_{1,4} = \left( \frac{A_{k_4}}{(I_{1,4} / Ip_4)^{C_{k_1}} - 1} + B_{k_1} \right) \times TDS_1$$

(Case 5: When fault occurs at place 5)

$$T_{2,5} = \left( \frac{A_{k_2}}{(I_{2,5} / Ip_2)^{C_{k_2}} - 1} + B_{k_2} \right) \times TDS_2$$

$$T_{1,5} = \left( \frac{A_{k_1}}{(I_{1,5} / Ip_1)^{C_{k_1}} - 1} + B_{k_1} \right) \times TDS_1$$

$$T_{1,5} - T_{2,5} \geq 0.2$$

(Case 6: When fault occurs at place 6)

$$T_{2,6} = \left( \frac{A_{k_2}}{(I_{2,6} / Ip_2)^{C_{k_2}} - 1} + B_{k_2} \right) \times TDS_2$$

$$T_{1,6} = \left( \frac{A_{k_1}}{(I_{1,6} / Ip_1)^{C_{k_1}} - 1} + B_{k_1} \right) \times TDS_1$$

$$T_{1,6} - T_{2,6} \geq 0.2$$

(Case 7: When fault occurs at place 7)

$$T_{3,7} = \left( \frac{A_{k_3}}{(I_{2,7} / Ip_2)^{C_{k_3}} - 1} + B_{k_3} \right) \times TDS_3$$

$$T_{1,7} = \left( \frac{A_{k_1}}{(I_{1,7} / Ip_1)^{C_{k_1}} - 1} + B_{k_1} \right) \times TDS_1$$

$$T_{1,7} - T_{3,7} \geq 0.2$$

(Case 8: When fault occurs at place 8)

$$T_{3,8} = \left( \frac{A_{k_3}}{(I_{3,8} / Ip_3)^{C_{k_3}} - 1} + B_{k_3} \right) \times TDS_3$$

$$T_{1,8} = \left( \frac{A_{k_1}}{(I_{1,8} / Ip_1)^{C_{k_1}} - 1} + B_{k_1} \right) \times TDS_1$$

$$T_{1,8} - T_{3,8} \geq 0.2$$

(Case 9: When fault occurs at place 9)

$$T_{3,9} = \left( \frac{A_{k_3}}{(I_{2,9} / Ip_3)^{C_{k_3}} - 1} + B_{k_3} \right) \times TDS_3$$

$$T_{1,9} = \left( \frac{A_{k_1}}{(I_{1,9} / Ip_1)^{C_{k_1}} - 1} + B_{k_1} \right) \times TDS_1$$

$$T_{1,9} - T_{3,9} \geq 0.2$$

(Relay time current characteristic curve selection constraints)

$$A_i = 0.0515 + K_{i,1} \times (19.61 - 0.0515) + K_{i,2} \times (28.2 - 0.0515) \quad \text{for } i = 1, 2 \text{ and } 3$$

$$B_i = 0.114 + K_{i,1} \times (0.491 - 0.114) + K_{i,2} \times (0.1217 - 0.114) \quad \text{for } i = 1, 2 \text{ and } 3$$

$$C_i = 0.02 + K_{i,1} \times (2.0 - 0.02) + K_{i,2} \times (2.0 - 0.02) \quad \text{for } i = 1, 2 \text{ and } 3$$

$$K_{i,1} + K_{i,2} \leq 1 \quad \text{for } i = 1, 2 \text{ and } 3$$

$$K_{i,1}, K_{i,2} = 0 \text{ or } 1$$

(Fuse saving scheme)

$$T_{3,7} \leq 0.06$$

$$T_{3,8} \leq 0.05$$

$$T_{3,9} \leq 0.06$$

### 3.5.3 Solution

The optimization problem is built in LINGO. Using MINLP formulation, the result is shown in Table 3.9. Considering the fuse saving scheme, recloser 2 can react in 0.02s which is much faster than the fuse blow process. And recloser 3 is capable to operate within 0.1s to avoid fuse blowing. With fuse saving process, reclosers and breakers are more sensitive to fault current so that long term power outages are greatly reduced at the sacrifice of increasing the momentary power outages.

Table 3.9 – Results for the optimal relay setting in IEEE 123 node system

Relay	TDS	Pickup Current	TC curve	Objective Value
Relay 1	0.1	173.8	Extremely Inverse	0.9604
Relay 2	0.1	35	Extremely Inverse	
Relay 3	0.1	70	Extremely Inverse	

# **CHAPTER 4**

## **AUTOMATIC SYSTEM RESPONSE**

### **4.1 Introduction**

Distribution system is the network which transfers the power from the transmission lines to the load centers over long distance. The distribution network consisting of feeders, transformers, loads, lines and protective devices is generally built as interconnected mesh network. While in operation, the network is arranged in the form of radial line structures, indicating that the systems are divided into a number of subsystems of radial feeders. Each feeder is divided into several load sections with closed sectionalizing switches and has connections to other feeders via several open tie switches. The main purpose of the sectionalizing switches is the isolation or restoration of loads during an outage or maintenance. As an outage occurs on the system, distribution networks must be reconfigured as quickly as possible to restore as much out-of-service loads as possible. Service restoration after an outage usually refers to an emergency situation.

Implementation of smart grid technologies will result in (a) more switching devices deployed in distribution systems and (b) a communication infrastructure that will provide information on status of switches / breakers and will also enable remote control of switches. The remote-controlled switches have become economically viable due to the large amount of automation suppliers and the arrival of new communication technologies. This arrangement will be ideal to support optimization and reconfiguration for the purpose of restoring power to customers.

Thus the objective of network reconfiguration is to maximize the amount of power restored and reduce the amount of time to restore the energy supply while the following constraints are satisfied,

- (i) voltage constraints,
- (ii) radiality constraints,
- (iii) line losses
- (iv) loading constraints and

Thus service restoration is a complicated combinatorial optimization problem because there are a great number of switches in the distribution system. It may take a long time to reach a feasible restoration plan which satisfies all the requirements. Therefore, the dispatchers at many utilities tend to use their experience to narrow down and reach a proper restoration plan in a short period.

## **4.2 Switch Placement Optimization**

It is obvious that smart switches are required to improve power system reliability, i.e., to reduce reliability indices. However, adding smart switches to the system is directly related to the increase in costs. Therefore, there exists a trade-off between power reliability improvement and costs. Then, the question is: What the optimal number of smart switches that leads to the minimal cost? Here, optimization techniques come in to play.

Figure 4.1 shows how the optimization of switch placement works. Initially, an optimization algorithm generates a set of random switch locations and feed it to the

power model. Then, pre-defined, random fault profiles are applied to the power system, which will eventually return back to normal, un-faulted conditions through the control model's switching algorithm. Once the power system returns to its normal conditions, SAIDI savings, which is the reduction in SAIDI scores by adding new switches, and related switch costs are calculated, both of which consist of the objective function. Based upon the value of the objective function, the optimization algorithm updates switch locations again and feeds them back to the power model until it reaches an optimum placement or until it is terminated by some criteria. We use two heuristic optimization techniques: Particle Swarm Optimization (PSO) and Genetic Algorithm (GA) Optimization.

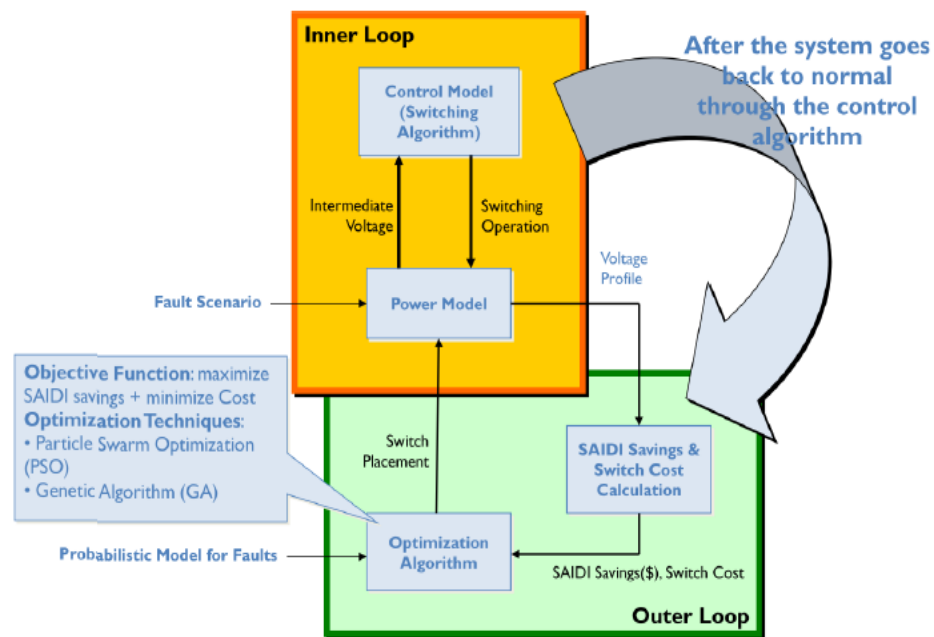


Figure 4.1 Switch Placement Optimization

Most general-purpose optimizations make use of gradient-based algorithms, mainly due to their computational efficiency. However, non-gradient-based, probabilistic optimization algorithms have attracted much attention from the research community.

Although these probabilistic optimization algorithms generally require many more function evaluations to find an optimum solution, as compared to gradient-based algorithms, they do provide several advantages. These algorithms are generally easy to program, can efficiently make use of large numbers of processors, do not require continuity in the problem definition, and are generally better suited for finding a global, or near global, solution. In particular, these algorithms are ideally suited for solving discrete and/or combinatorial-type optimization problems.

There are several modern heuristic optimization techniques such as evolutionary computation, simulated annealing, tabu search, particle swarm, etc. Recently, genetic algorithm (GA) and particle swarm optimization (PSO) techniques appeared as promising algorithms for handling the optimization problems because of their versatility and ability to optimize in complex multimodal search spaces applied to non-differentiable objective functions. Both GA and PSO are similar in the sense that they are population-based search methods and they search for the optimal solution by updating generations.

While GA is inherently discrete, i.e., it encodes the design variables into bits of 0's and 1's, and therefore easily handles discrete design variables, PSO is inherently continuous and must be modified to handle discrete design variables.

#### **4.2.1 Problem Formulation**

##### **Objective Function**

The objective function consists of two parts: one is to maximize SAIDI savings that we can obtain by applying a new set of switches to the power system, and the other is to minimize the cost related to those new switches. This can be expressed by

$$\max_x f(x) = (SAIDI\_Savings - Switch\_Cost)$$

Where  $x$  is a switch placement. The following steps describe how each term is derived:

1. Switch Cost is calculated based on the number of switches used and the number of phases in each switch. It is assumed that the cost of a single-phase switch is \$2,500, the cost of a three-phase switch is \$5,500, and the cost of a two-phase switch is twice that of a single-phase switch, \$5,000.
2. Total Possible SAIDI Minutes is calculated by dividing Total Sustained Fault Time in Profile times  $N_T$  by  $N_T$ , where  $N_T$  is the total number of customers served in an area.
3. Total SAIDI minutes saved is calculated by subtracting total SAIDI minutes experienced from total possible SAIDI minutes.
4. Annual Average % SAIDI Reduction is calculated by dividing SAIDI Minutes Saved by Total Possible SAIDI Minutes.
5. Annual Average % SAIDI Reduction is converted to a Total \$ Savings amount by using the estimated fault cost per SAIDI minute calculated from the Lawrence Berkeley National Labs corresponding interest rate taken from current US t-bond rate by varying the payback period, the weighting of switch cost vs. SAIDI benefits changes.

6. The objective function is calculated as: Total \$ Savings from SAIDI Reduction – Total Switch Cost, and this value is to be maximized.

### **Representation of Switches**

Basically, the IEEE Node-123 Test Feeder has 120 buses where a smart switch can be added. Those 120 buses are represented by a  $1 \times 120$  binary string, of which each bit represents whether a switch is attached to the corresponding bus. If a bit is set to 0, there is no additional switch on the bus; if a bit is set to 1, then a switch is added to the bus. This binary string can be directly applied to a GA because it is inherently a discrete optimization technique; however, since PSO is a continuous optimization technique, the particles of a PSO need to be expressed in a binary string.

### **4.2.2 Particle Swarm Optimization**

Particle swarm optimization (PSO) is one of the evolutionary computation techniques motivated by the simulation of social behavior. PSO was developed by Kennedy and Eberhart in the mid 1990s. It is a population-based search algorithm and is initialized with a population of random solutions, called particles. PSO is similar to genetic algorithm (GA) in that the system is initialized with a population of random solutions. It is unlike GA, however, in that each potential solution is also assigned a randomized velocity, and each particle flies over the search space at velocity dynamically adjusted according to the historical behaviors of the particle and its companions.

Key Features of Particle Swarm Optimization [8]:

- It uses function values only.

- It requires relatively little fine tuning.
- It is easy to program.
- It requires a very large number of function evaluations. However, if approximation techniques are used, this may be offset by the fact that function evaluations are very fast.

#### 4.2.2.1 PSO Algorithm

PSO makes use of a velocity vector to update the current position of each particle in the swarm. The position of each particle is updated based on the social behavior that a population of individuals, the swarm in the case of PSO, adapts to its environment by returning to promising regions that were previously discovered [9]. The process is stochastic in nature and makes use of the memory of each particle, as well as the knowledge gained by the swarm as a whole. The outline of a basic PSO algorithm is as follows:

1. Start with an initial set of particles, typically randomly distributed throughout the design space.
2. Calculate a velocity vector for each particle in the swarm.
3. Update the position of each particle, using its previous position and the updated velocity vector.
4. Go to step 2 and repeat until convergence.

The scheme for updating the position of each particle is  $x_{k+1}^i = x_k^i + v_{k+1}^i$

Where  $x_{k+1}^i$  is the position of the particle  $i$  at the iteration  $k+1$  and  $v_{k+1}^i$  is the

corresponding velocity vector.

The scheme for updating the velocity vector of each particle depends on the particular PSO algorithm under consideration. A commonly used scheme, introduced by Shi and Eberhart [10], is

$$v_{k+1}^i = wv_k^i + c_1r_1(p^i - x_k^i) + c_2r_2(p_k^g - x_k^i)$$

Where  $r_1$  and  $r_2$  are independent random numbers between 0 and 1,  $p^i$  is the best position found by particle  $i$  so far, and  $p_k^g$  is the best position in the swarm at time  $k$ . There are three problem-dependent parameters, the inertia of the particle  $w$  and two ‘trust’ parameters  $c_1$  and  $c_2$ , which regulate the relative velocity toward local and global best, respectively. The inertia controls the exploration properties of the algorithm, with larger values facilitating a more global behavior and smaller values facilitating a more local behavior. It is indicated in [10] that decreasing the inertia weight from about 0.9 to 0.4 during an optimization run provides improved performance in a number of applications. The trust parameters indicate how much confidence the current particle has in itself,  $c_1$ , and how much confidence it has in the swarm,  $c_2$ . In [10] it is proposed that using  $c_1=c_2=2.05$  for multimodal functions will provide improved optimization performance.

Clerc in [11] indicates that use of a constriction factor may be necessary to insure convergence of the particle swarm algorithm. A simplified method of incorporating a constriction factor appears in the equation

$$v_{k+1}^i = K \left[ wv_k^i + c_1 r_1 (p^i - x_k^i) + c_2 r_2 (p_k^g - x_k^i) \right]$$

Where  $K$  is the a function of  $c_1$  and  $c_2$  as in the equation:

$$K = \frac{2}{\left| 2 - \varphi - \sqrt{\varphi^2 - 4\varphi} \right|}, \varphi = c_1 + c_2, \varphi > 4$$

A maximum allowable velocity vector  $V_{\max}$  clamps velocities of particles on each dimension. If the acceleration causes the velocity on a dimension to exceed  $V_{\max}$  specified by the user, then the velocity on that dimension is limited to  $V_{\max}$ .

Eberhart and Shi compared the performance of PSO with its different versions, and concluded that the best approach is to use the constriction factor while limiting the maximum velocity  $V_{\max}$  to the dynamic range of the variable  $X_{\max}$  on each dimension [10]. In this work, the PSO algorithm described in [9] and [11] is implemented.

#### 4.2.2.2 Implementation of PSO

##### **Optimization Parameters**

The inertia weight ( $w$ ) is set to 0.9 at the beginning of the run, and made to decrease linearly to 0.4 at the maximum number of iterations.  $V_{\max}$  is set to maximum range  $X_{\max}$ . Each of the two ( $p-x$ ) terms is multiplied by acceleration constants,  $c_1$  and  $c_2$ , of 2.05 (times a random number between 0 and 1). Also, Clerc's constriction method is used.  $\varphi$  is set to 4.1 and the constant multiplier  $K$  is thus 0.729, and each of the two ( $p-x$ ) terms being multiplied by  $0.729 \times 2.05 = 1.49445$  (times a random number between 0

and 1). From [10],  $V_{\max}$  is set to be equal to  $X_{\max}$ . This significantly improves results when using the constriction approach, creates the most consistent way to obtain good results, and almost always creates the fastest optimization [10].

### **Initial Swarm**

The initial swarm is generally created such that the particles are randomly distributed throughout the design space, each with a random initial velocity vector. The following equations are used to obtain the random initial position and velocity vectors:

$$x_0^i = X_{\min} + r_3(X_{\max} - X_{\min})$$

$$v_0^i = X_{\min} + r_4(X_{\max} - X_{\min})$$

where  $x_0^i$  is the initial position vector,  $v_0^i$  is the initial velocity vector of particle  $i$ ,  $r_3$  and  $r_4$  are independent random numbers between 0 and 1,  $X_{\min}$  is the vector of lower bounds, and  $X_{\max}$  is the vector of upper bounds for the design variables.

The initial swarm distribution has an influence on the effectiveness of the PSO algorithm; however, the influence of the initial swarm distribution is not important, as long as it is fairly well distributed throughout the design space [9]. In this work, all initial swarms were randomly distributed.

#### 4.2.2.3 Procedures of the PSO

The following is the procedure of the PSO we implemented, from [12]:

1. Initialize a population of  $N$  particles. For the  $i$ th particle, its location  $x_i$  in the search

space is randomly placed. Its velocity vector is  $v_i$  in which the velocity in the  $d$ th dimension is  $v_{id} = rand \times V_{max}$ , where is the random number in the range of (-1, 1).

2. Assign  $\varphi$ . Calculate  $K$ , and assign  $c_1 = c_2 = \varphi / 2$ .
3. Set the number of iteration  $k=1$ , and evaluate the fitness function for each particle. Let  $p_{best}$  equal the fitness value of each particle. Let  $g_{best}$  equal the index of the particle which gives best fitness value.
4. Compare the evaluated fitness value of each particle with its  $p_{best}$ . If the current value is better than  $p_{best}$ , then set the current location as the  $p_{best}$  location.
5. Furthermore, if the current value is better than  $g_{best}$ , then reset  $g_{best}$  to the current index in the particle array.
6. Change the velocity and location of the particles according to the equations, respectively. Check if the velocity and location exceed the constraints.
7. Set  $k=k+1$ , repeat Steps 4-5 until the number of iteration is greater than the allowable maximum iteration number  $T_{max}$ .

#### 4.2.2.4 Validation of PSO Algorithm

The implemented PSO algorithm was applied to a sample optimization problem involving a two design variable, unconstrained mathematical function. The objective function to be minimized is shown below, with the two design variables allowed to vary between -50 and 10:

$$F(x_1, x_2) = x_1^2 - 100(\cos x_1)^2 - 100(\cos x_1^2 / 30) + x_2^2 - 100(\cos x_2)^2 - 100(\cos x_2^2 / 30) + 1400$$

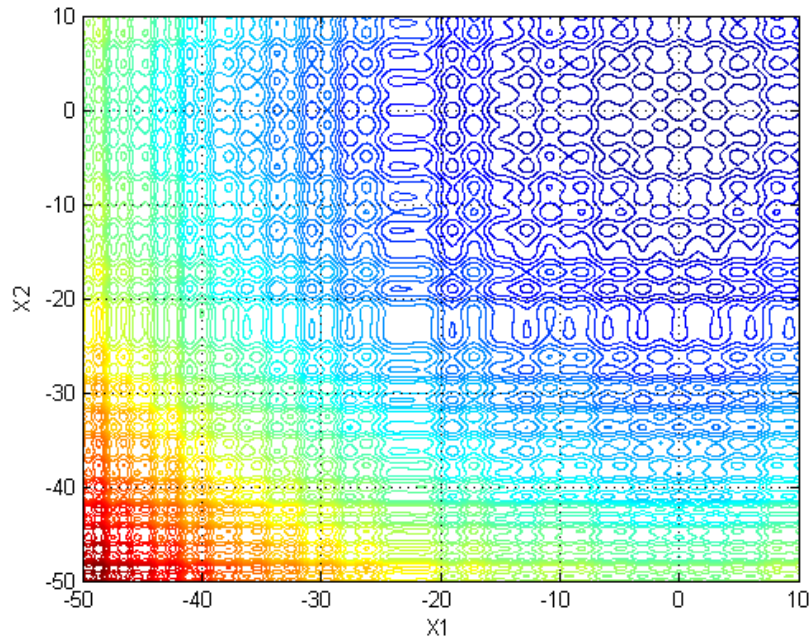


Figure 4.2 Contour plot of sample objective function

This function has many local minima, and the global optimum has a value of 1000 at  $x_1 = x_2 = 0$  as shown in Figure 4.2 above. A swarm sizes of 20 particles, was considered with  $c_1=1.5$  and  $c_2=2.5$ , and the craziness operator was applied. The optimization was repeated 50 times and the best, worst, mean, and standard deviation of the best objective function and the number of function evaluations to convergence were calculated for each of 50 repetitions. In addition, the reliability of the algorithm, measured in terms of the success rate by counting the number of optimization runs that found an objective function value within 1% of the best objective function value from all 50 runs, was also calculated. The results are summarized in Table 4.1 and Table 4.2.

Table4.1 - Number of function evaluation for continuous case

Mean	Standard Deviation	Best	Worst
1966	240	300	2000

Table 4.2 - Objective function for continuous case

Mean	Standard Deviation	Best	Worst	Success Rate, %
1000.35	2.47	1000.00	1017.43	98.00

The results of Table 4.1 and Table 4.2 clearly show that the implemented PSO algorithm is capable of solving the unconstrained, continuous example problem very accurately. It is also able to deal with the many local minima present in the objective function and finds the global optimum reliably.

Furthermore, to see if the implemented PSO can deal with integer design variables like in our formulation of the switch placement optimization, the design variables were converted to integers and the PSO algorithm was applied to the integer design variable optimization problem. The simulation results are summarized in Table 4.3 and Table 4.4.

Table 4.3 - Number of function evaluation for integer case

Mean	Standard Deviation	Best	Worst
1660	686	240	2000

Table 4.4 - Objective function for integer case

Mean	Standard Deviation	Best	Worst	Success Rate, %
1005.24	18.02	1000.00	1123.03	80.00

As shown in Table 4.3 and Table 4.4, the implemented PSO can also deal with the integer design variable reliably like as in the continuous case. Therefore, the implemented PSO algorithm is validated to deal with both continuous and integer design variable

problems. Figure 4.3 shows how particles fly over the design space to get to the optimum value at  $x_1 = x_2 = 0$ . The blue circles represent the initial particles and the red crosses represent the final position of the particles. It can be seen that particles, which are initially scattered in the design space, flock together at the optimum point through the implemented PSO algorithm.

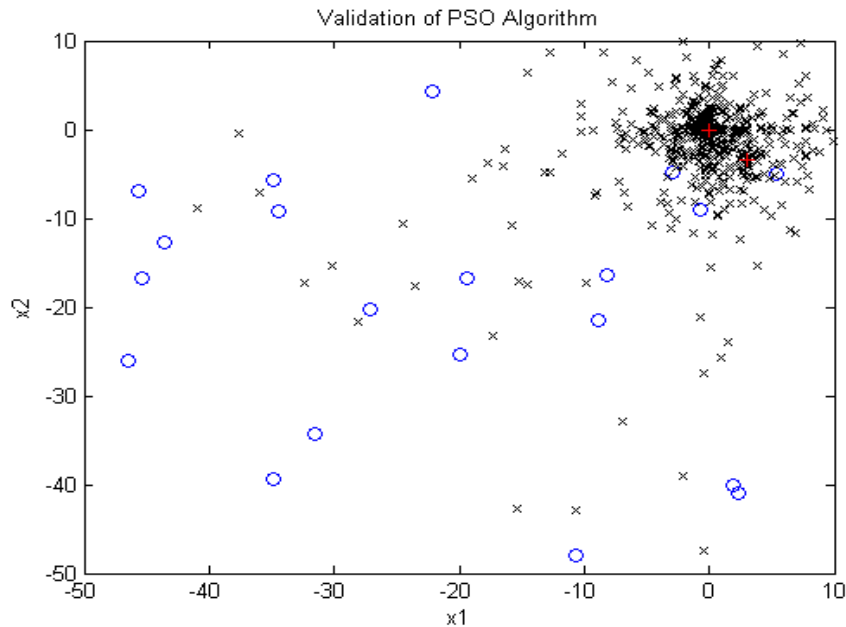


Figure 4.3 Validation of PSO Algorithm

#### 4.2.2.5 Verification of the PSO Algorithm for Switch Placement Optimization

In order to verify the implemented PSO algorithm, two simple cases are optimized; the first involves adding 1 switch to the system and the second involves adding 2 switches in the system. To see if the PSO algorithm is capable of finding a “near-optimal” switch placement, the theoretical optimal solution is required. Since there are only 120 possible ways to add 1 switch and 7140 ways to add 2 switches, to find a theoretical optimum for both cases is quite simple by brute force, and thus the switch placement optimizations of 1 switch and 2 switches are considered to verify the

implemented algorithm. The other cases are not considered because due to exponentially increasing simulation times; for example, if 3 switches are to be added, then there are over 280 thousand cases to be run to find a theoretical optimum solution, as calculated below.

$$\frac{120!}{(120-3)!3!} = 280840$$

For the purpose of finding the theoretical optimum, the objective function, SAIDI reduction, and cost for all the possible switch location were first simulated by adding a switch or two switches to all possible buses of the IEEE Node-123 Test Feeder and running the power model. Table 4.5 compares both cases.

Table 4.5 - Comparison of 1-switch and 2-switch simulations

No. of switches	No. of possible placement	No. of Fault Profiles Applied	Payback Period	Interest Rate	Switch Cost
1	120	119	1 year	0.30%	\$2,500/1-phase \$5,000/2-phase
2	7140	1	1 year	0.30%	\$5,500/3-phase

Table 4.6 summarizes the objective function (i.e. FVAL), SAIDI reduction, and switch cost against the switch location for the 1-switch case (Payback Period: 1 year; Interest Rate: 0.30%). Note that Table 4.6 shows the benefits, SAIDI reduction, and cost which can be obtained by adding a switch to all the possible bus location, not optimization results. As seen in Table 4.6, for the 1-switch case, adding a switch to Bus 58 has the most benefit, that is, Bus 58 is the theoretical, optimum location of a new switch.

Table 4.6 - Fval, SAIDI Reduction, & Cost of 1-Switch Verification Case

PO S	FVAL	SAIDI(%)	SAIDI(\$)	COS T	PO S	FVAL	SAIDI(%)	SAIDI(\$)	COS T
1	-5458.77	0.0003	41.23	5500	61	-2436.66	0.0005	63.34	2500
2	13137.83	0.1357	18637.83	5500	62	-2435.53	0.0005	64.47	2500
3	-2435.53	0.0005	64.47	2500	63	286.75	0.0421	5786.75	5500
4	3057.85	0.0405	5557.85	2500	64	63.33	0.0405	5563.33	5500
5	-2436.65	0.0005	63.35	2500	65	62072.13	0.4919	67572.13	5500
6	3149.4	0.0411	5649.4	2500	66	154.88	0.0412	5654.88	5500
7	3195.21	0.0415	5695.21	2500	67	246.42	0.0418	5746.42	5500
8	14032.36	0.1422	19532.36	5500	68	256.84	0.0419	5756.84	5500
9	23778.06	0.2131	29278.06	5500	69	276.34	0.042	5776.34	5500
10	3057.85	0.0405	5557.85	2500	70	43031.92	0.3533	48531.92	5500
11	-2435.53	0.0005	64.47	2500	71	29426.06	0.2542	34926.06	5500
12	3149.4	0.0411	5649.4	2500	72	3012.05	0.0401	5512.05	2500
13	52626.65	0.4231	58126.65	5500	73	3057.85	0.0405	5557.85	2500
14	63212.42	0.5002	68712.42	5500	74	3149.4	0.0411	5649.4	2500
15	3057.85	0.0405	5557.85	2500	75	3195.21	0.0415	5695.21	2500
16	3195.21	0.0415	5695.21	2500	76	39278.63	0.326	44778.63	5500
17	-2435.53	0.0005	64.47	2500	77	-2441.16	0.0004	58.84	2500
18	3195.21	0.0415	5695.21	2500	78	-2438.91	0.0004	61.09	2500
19	-2435.53	0.0005	64.47	2500	79	-2436.65	0.0005	63.35	2500
20	22990.46	0.2074	28490.46	5500	80	-262.59	0.0381	5237.41	5500
21	19494.28	0.1819	24994.28	5500	81	22186.75	0.2015	27686.75	5500
22	-2438.91	0.0004	61.09	2500	82	-171.04	0.0388	5328.96	5500
23	-2436.65	0.0005	63.35	2500	83	-5436.65	0.0005	63.35	5500
24	16733.37	0.1618	22233.37	5500	84	-79.5	0.0395	5420.5	5500
25	-2436.65	0.0005	63.35	2500	85	12.05	0.0401	5512.05	5500
26	14946.01	0.1488	20446.01	5500	86	-5437.78	0.0005	62.22	5500
27	-2436.65	0.0005	63.35	2500	87	-2437.78	0.0005	62.22	2500
28	1000.21	0.0473	6500.21	5500	88	-5486.66	0.0001	13.34	5500
29	6146.1	0.0811	11146.1	5000	89	-2436.65	0.0005	63.35	2500
30	-4936.65	0.0005	63.35	5000	90	16733.37	0.1618	22233.37	5500
31	3195.14	0.0415	5695.14	2500	91	13158.65	0.1358	18658.65	5500
32	-2436.65	0.0005	63.35	2500	92	-2436.65	0.0005	63.35	2500

Table 4.6 continued

33	-1144.66	0.0317	4355.34	5500	93	11371.29	0.1228	16871.29	5500
34	-3289.53	0.0161	2210.47	5500	94	-2436.65	0.0005	63.35	2500
35	-5434.4	0.0005	65.6	5500	95	4220.42	0.0708	9720.42	5500
36	-2435.53	0.0005	64.47	2500	96	-2436.65	0.0005	63.35	2500
37	3149.4	0.0411	5649.4	2500	97	2254.3	0.0564	7754.3	5500
38	15583.37	0.1535	21083.37	5500	98	-2436.65	0.0005	63.35	2500
39	603.59	0.0408	5603.59	5000	99	3240.95	0.0418	5740.95	2500
40	-2436.65	0.0005	63.35	2500	100	1000.21	0.0473	6500.21	5500
41	-2436.66	0.0005	63.34	2500	101	9567.63	0.1097	15067.63	5500
42	-2435.53	0.0005	64.47	2500	102	-1144.66	0.0317	4355.34	5500
43	10461.16	0.1162	15961.16	5500	103	-3289.53	0.0161	2210.47	5500
44	3240.95	0.0418	5740.95	2500	104	-5434.4	0.0005	65.6	5500
45	-2436.65	0.0005	63.35	2500	105	5013.1	0.0765	10513.1	5500
46	10866.46	0.1191	16366.46	5500	106	-2440.04	0.0004	59.96	2500
47	5611.41	0.0809	11111.41	5500	107	-2438.91	0.0004	61.09	2500
48	3195.14	0.0415	5695.14	2500	108	-2436.65	0.0005	63.35	2500
49	3240.95	0.0418	5740.95	2500	109	-33.76	0.0398	5466.24	5500
50	-5435.12	0.0005	64.88	5500	110	3103.66	0.0408	5603.66	2500
51	5698.07	0.0815	11198.07	5500	111	-2436.65	0.0005	63.35	2500
52	5736.58	0.0818	11236.58	5500	112	-5434.4	0.0005	65.6	5500
53	5917.42	0.0831	11417.42	5500	113	2966.24	0.0398	5466.24	2500
54	286.75	0.0421	5786.75	5500	114	3057.79	0.0405	5557.79	2500
55	63212.61	0.5002	68712.61	5500	115	3240.95	0.0418	5740.95	2500
56	63212.8	0.5002	68712.8	5500	116	-2438.91	0.0004	61.09	2500
57	195.14	0.0415	5695.14	5500	117	-2437.78	0.0005	62.22	2500
58	63537.04	0.5026	69037.04	5500	118	-2435.53	0.0005	64.47	2500
59	240.95	0.0418	5740.95	5500	119	-2434.4	0.0005	65.6	2500
60	63358.35	0.5013	68858.35	5500	120	-5434.4	0.0005	65.6	5500

For the 2-switch case fifty-six different 2-switch combinations show the maximal economic benefits, which is about \$120K under the assumption of 1-year payback period and an interest rate of 0.30%. Due to its enormous size, the simulation result for finding a theoretical optimum of the 2-switch case is not included in this report. In order to reduce the optimization run time, a simplified set of fault scenarios was applied to the 2-switch case while a comprehensive set of 119 fault profiles was applied to the 1-switch case. For both cases, 100 optimization runs were performed.

**Optimization Results of the 1-Switch Case**

The verification results are summarized in Table 4.7 (Payback Period: 1 year; Interest Rate: 0.30%) and Table 4.8 (Payback Period: 1 year; Interest Rate: 0.30%). Of 100 runs, 98 runs yield Bus 58 as an optimum location of switch. Two runs found Bus 60 as an optimum location for a new switch; in other words, the success rate is 98%. However, Bus 60 is a near-optimum location as indicated by the standard deviation of \$25.14 in Table 4.8.

Table 4.7 - Number of Function Evaluations of 1-Switch PSO Optimization

Mean	Standard Deviation	Best	Worst
679,728	152,199.75	523,600	1,142,400

Table 4.8 - Objective Function of 1-Switch PSO Optimization

Mean	Standard Deviation	Best	Worst	Success Rate, %	Optimum Location
\$63,533.47	\$25.14	\$63,537.04	\$63,358.35	98.00	Bus#58

Since 119 fault profiles were applied to the SAIDI reduction calculation of each particle, 119 function evaluations are required to evaluate a particle's objective function. Hence, 2380 (=119\*20) function evaluations are required for 20 particles. This is why the number of function evaluations is so large. Based upon these results, even though the standard deviation of function evaluations is quite large, the implemented PSO algorithm is capable of finding an optimum switch placement with great accuracy.

### **Optimization Results of the 2-Switch Case**

The optimization results of the 2-switch case are summarized in Table 4.9 (Payback Period: 1 year; Interest Rate: 0.30%) and Table 4.10 (Payback Period: 1 year;

Interest Rate: 0.30%).

Table 4.9 - Number of Function Evaluations of 2-Switch PSO Optimization

Mean	Standard Deviation	Best	Worst
511.2	81.7150	440	920

Table 4.10 - Objective Function of 2-Switch PSO Optimization

Mean	Standard Deviation	Best	Worst	Success Rate, %	Optimum Location
\$120,760.00	\$184.00	\$120,792.20	\$ 119,718.99	97.00	56 Unique Switch Combinations

Like the 1-switch case, the implemented PSO algorithm finds an optimum solution very accurately. Of 100 optimization runs, only 3 runs found very different locations which, however, are near-optimum solutions as indicated by the standard deviation of \$184.00 in Table 4.10.

#### 4.2.2.6 Conclusion of the PSO Algorithm Verification

The IEEE 123 Node Test Feeder is similar to the simple mathematical function in that it has multiple local maxima; however, it differs from the simple mathematical function in the sense that it doesn't have near-optimal solutions around its local optima. Therefore, it was not possible to observe that each particle representing switch locations flies towards the optimum solution, and it is also not possible to display simulation results in a figurative way as shown in Figure 4.4 (red line: optimal location, black circles: best locations at every iteration, blue star: particles' positions at every iteration). The implemented PSO algorithm shows a behavior similar to one of a general random search. That's the reason in this work the inertia coefficient  $w$  was changed to 1.4, not

dynamically decreased from 0.9 to 0.4, in order to ensure a global search.

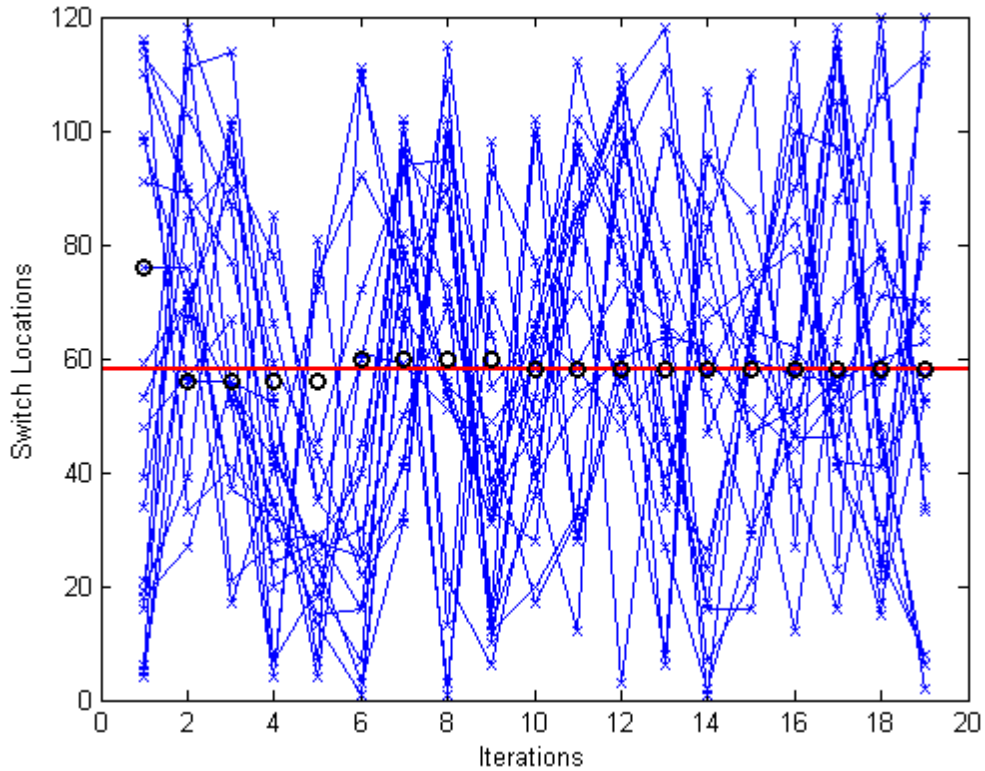


Figure 4.4 Verification of PSO Algorithm with 1 Switch

### Initial Optimization Results of PSO Algorithm

First, for simplicity, only 10 random, but pre-defined, fault profiles were applied and the switch placement was optimized using the implemented PSO algorithm under the assumption of 2-year payback period and the interest rate of 0.61%.

To find the optimum switch placement, the PSO algorithm optimized the switch placement for each number of switches varying from 2 to 15. After the optimum switch placement for each number of switches had been obtained, the optimum number of switches which provides the highest benefits was determined off-line among those 14

optimization results. Table 4.11 (Payback Period: 2 years; Interest Rate: 0.61%) summarizes the optimization results with 10 fault profiles.

Table 4.11 - Optimization Results of PSO with 10 Fault Profiles

No. of Switches	Benefits (\$)	SAIDI Reduction (%)
2	159,290	62.07
3	169,010	67.62
4	171,890	69.58
5	179,450	73.25
6	182,620	77.51
7	184,720	79.18
8	176,960	77.08
9	179,180	80.08
10	189,190	84.46
11	171,590	79.13
12	169,860	81.60
13	163,680	79.17
14	172,340	83.23
15	172,990	88.57

The PSO algorithm yielded 10 switches as an optimum number of switches that gives the highest benefit, \$189,190; however, 15 switches gives better SAIDI reduction. The reason why 15-switch provides the more SAIDI reduction with the lower benefits is that the increase in the number of switches added to the power system not only reduces the SAIDI more but also increase the switch cost. It is obvious as shown in Table 4.12: the addition of 120 switches dramatically reduces the SAIDI score, which is almost 98% reduction, but the switch cost also dramatically increases so as to have an adverse effect on the benefits.

Table 4.12: Objective Function, SAIDI Reduction, and Cost of 120-Switch Case

Payback Period	Interest Rate	Benefits (\$)	SAIDI Reduction (%)	SAIDI Reduction (\$)	Switch Cost (\$)
1 Year	0.30%	-356,032.94	97.88	134,467.06	490,500.00
2 Years	0.61%	-223,207.28	97.88	267,292.72	490,500.00

Figure 4.5 (Payback Period; 2 years; Interest Rate: 0.61%) and Figure 4.6 (Payback Period; 2 years; Interest Rate: 0.61%) below show the benefits (objective function) and SAIDI reduction against the number of switches with 10 fault profiles applied, respectively. It can be also seen in Figure 4.6 that the more switches are added to the system, the more reduction in SAIDI scores can be achieved.

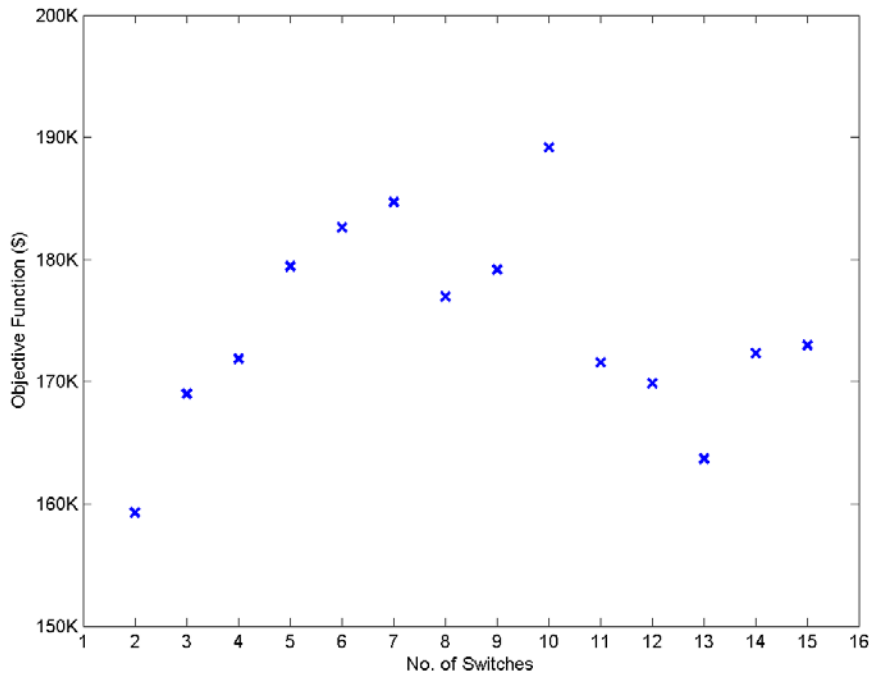


Figure 4.5 Objective Function of 1-Switch PSO Optimization

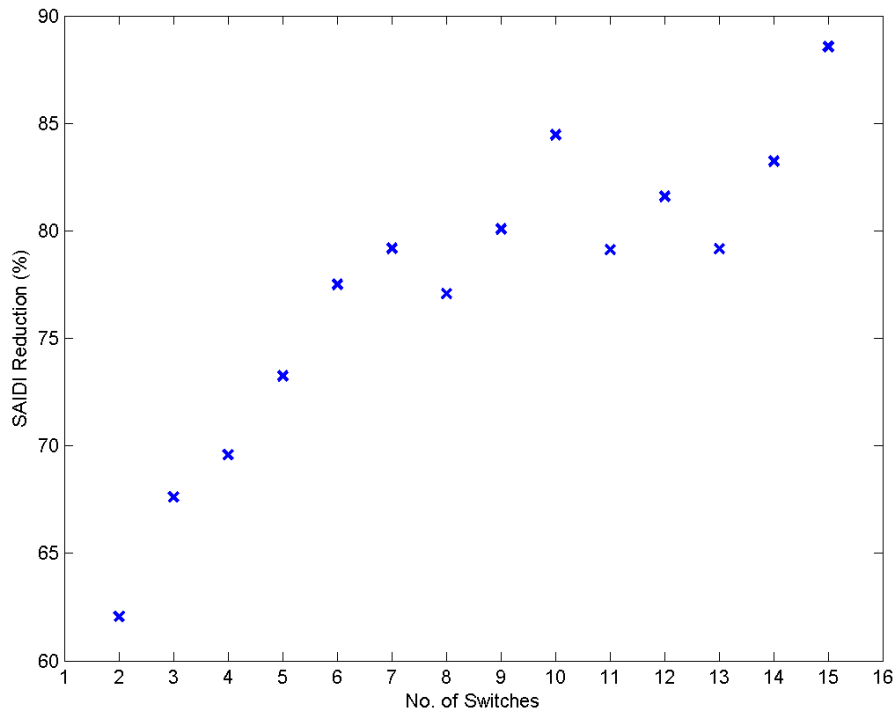


Figure 4.6 SAIDI Reduction of 1-Switch PSO Optimization

### 4.2.3 Genetic Algorithm

Genetic algorithms are an optimization method that employs a search process imitated from the mechanism of biological selection and biological genetics. They combine survival of the fittest among those feasible solutions in the form of string structures (or genes: in binary form), and a randomized formation exchange to form a search algorithm [13]. In every generation, a new set of solutions is created from the fittest of the previous set of solutions.

The control variables have to be represented as strings. During the search process, solutions are initially randomized. Then, the fitness of each solution is computed. The solution with higher fitness has higher probability to be chosen for generating a new

generation. This procedure is called reproduction or selection. A crossover is used for innovating of solutions, and a mutation can help solutions have a wider range of feasible solutions. After these three genetic operations, the new generation is obtained and it starts the genetic operations again and again until the optimum solution is found.

Key Features of Genetic Algorithms [9]:

- It uses function values only.
- It naturally handles discrete variable.
- It is easy to program.
- It requires a very large number of function evaluations. However, if approximation techniques are used, this may be offset by the fact that function evaluations are very fast.

#### 4.2.3.1 Implementation of a GA

##### **Representation**

The representation scheme determines how the problem is structured in a GA and also determines the genetic operators that can be used. For this study, a binary representation is used. IEEE Node-123 Test Feeder model has 120 line segments on which a smart switch is possibly added. We represent these 120 segments by a  $120 \times 1$  vector of which each bit represents whether a switch is added on a line segment or not. If a bit is set to 1, then the corresponding line segment will have a new switch; otherwise, it has no switch.

##### **Initialization of a Population**

A GA must be provided with an initial population. In the initial stage of the GA, a matrix of random switch locations with the number of rows equal to the population size and the number of columns equal to the number of the line segments on which a new switch can be added is created. A total population size of 80, which was recommended in [14], is used.

### Selection

The selection determines which of the individuals will survive and continue on to the next generation. The GA carries out the selection each generation after all the new children have been evaluated to create a new population from the old one. In this work, two selection techniques are considered: one is the Elitest technique and the other is to use a Roulette Wheel. The Elitest technique is to choose the predefined number of individuals that have the best fitness values. On the other hand, the Roulette Wheel technique uses a roulette wheel, each area of which is proportional to each individual's fitness, selects individuals on the portions of which randomly generated numbers fall. Thus, it prevents the algorithm from being trapped in local optima. Figure 4.7 illustrates how differently these two techniques work.

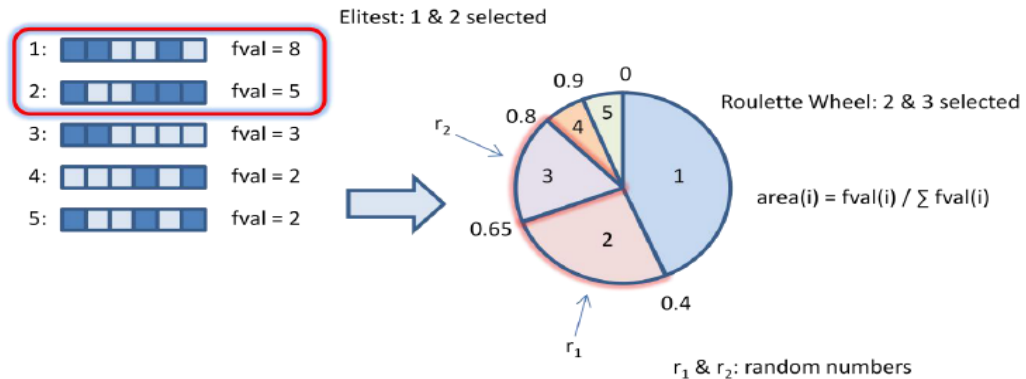


Figure 4.7 Selection - Elitest vs. Roulette Wheel

## Reproduction

To produce a new generation, two genetic operators, two-point crossover and non-uniform mutation, are used. From Figure 4.7, it is best in an off-line GA optimization for 90% of the new generation to be created by crossover and mutation, while 10% be carried over exactly from the previous generation.

## Crossover

Crossover takes two individuals and produces two new as individuals, as illustrated in Figure 4.8, where  $r_1$  and  $r_2$  are randomly generated numbers. From Figure 4.7, 45% of the members of the next generation should be created by crossover in an off-line GA optimization.

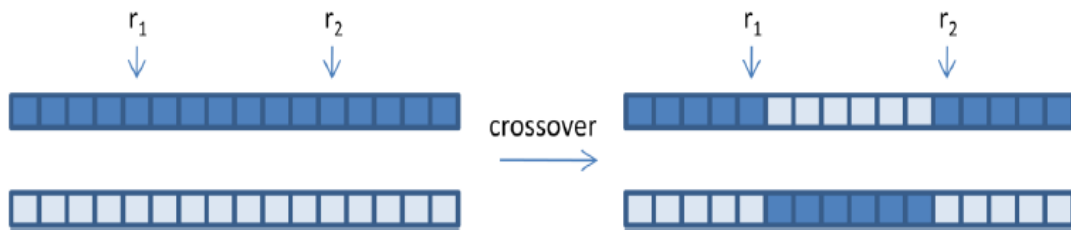


Figure 4.8 Two-Point Crossover

## Termination

The termination determines when to stop the simulated evolution and return the resulting switch placement. A maximum generation criteria is used to stop a simulation. A maximum generation of 50 is used.

## Mutation

Mutation alters one individual to produce a single new solution as illustrated in Figure 4.9 below. From Figure 4.7, the probability of any specific bit being mutated is set

to 0.01.

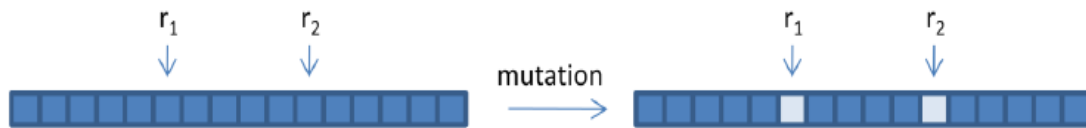


Figure 4.9 Mutation

#### 4.2.3.2 Procedures of the GA

The basic genetic algorithm implemented in this work consists of the following steps [8]:

1. Create a random initial population.
2. Calculate all fitness values.
3. Get the sum of all the fitness values  $F_{sum} = \sum F_i$ .
4. Construct a roulette wheel, with each binary string occupying an area on the wheel in proportion to the ratio  $F_i / F_{sum}$ .
5. Send 10% of the current population to the next generation unaltered, using the roulette wheel to choose, and always including the fittest individual. Note: Here a combination of the 'roulette wheel' and elitist strategies is employed.
6. For the remaining members of the next generation, use a random number 0-1 to pick pairs on the wheel as 'mating pairs' that will reproduce.
7. Perform crossover. Use a weighted coin toss to pick the probability of crossover, with the probability of crossover being 0.45.
8. If crossover is dictated, pick two integer numbers between 1 and the length of the

binary string to establish the starting and ending crossover locations. Exchange values in the string between parents.

9. Perform the mutation operation on the child, with the probability of mutation being 0.01 for every bit.

10. Repeat the process until convergence is achieved.

#### 4.2.3.3 Comparison of PSO and GA

Table 4.13 summarizes how differently the PSO and the GA optimization algorithm are implemented in this work. Both of them are applied to the IEEE Node-123 Test Feeder and have the same objective function, maximize the difference between SAIDI savings and related switch cost. However, the PSO can optimize only switch locations with the fixed number of switches because, if the number of switches varies, it can't update its particles' velocities and positions during optimization runs while the GA can optimize both switch locations and the number of switches simultaneously. In other words, the GA can take into account reliability indices and cost at the same time, but the PSO can consider cost off-line after all optimizations for a various number of switches are done. Due to the same reason, the representations of design variables are different. For the PSO, a  $120 \times 1$  binary string can have only the fixed number of 1's. On the other hand, the GA has a  $120 \times 1$  binary string which can have varying number of 1's. The same convergence criteria are applied to both techniques: an optimization process is terminated if it seems to converge to an optimal switch placement or if the maximum number of iterations is reached. The outcome of the optimization process is optimized switch location for the PSO and optimized number of switches and their locations for the GA.

Table 4.13 - Comparison of PSO and GA

	Optimization Techniques	
	Particle Swarm Optimization (PSO)	Genetic Algorithm (GA)
System Optimized	IEEE Node-123 Test Feeder	
Objective Function	Maximize SAIDI Savings + Minimize Cost	
Design Variables	Switch Locations	Switch Locations + No. of Switches
Design Variable Representation	$X = X_1, \dots, X_m$ $m$ : number of switches, $X_i$ : bus ID	$X = [X_1, \dots, X_n]$ $n$ : max. number of switches, $X_i = 0$ or 1
Optimization Approach	<ul style="list-style-type: none"> <li>Perform the optimization for every possible number of switches</li> <li>Find the best solution off-line based upon cost</li> </ul>	Optimize the number and location of switches at the same time
Convergence Criteria	Max. No. of Iterations or No More Improvements	
Outcomes	Optimized Switch Location	Optimized Number & Locations of Switches

#### 4.2.4 Results and Conclusions

From our genetic algorithm, the result given by the best found switch placement is shown in Table 4.14 below.

Table 4.14 - Optimal GA Switch Configuration Results

Payback Period	Interest Rate	Net Present Value of Benefits (\$)	SAIDI Reduction (%)	Annual SAIDI Savings (\$)	Switch Costs (\$)
1 Year	0.30%	84,238.50	81.3	111,404.50	27,500

Five switches need to be added to our baseline system, with the locations chosen by the GA as shown in Figure 4.10 below, in order to achieve to above results.

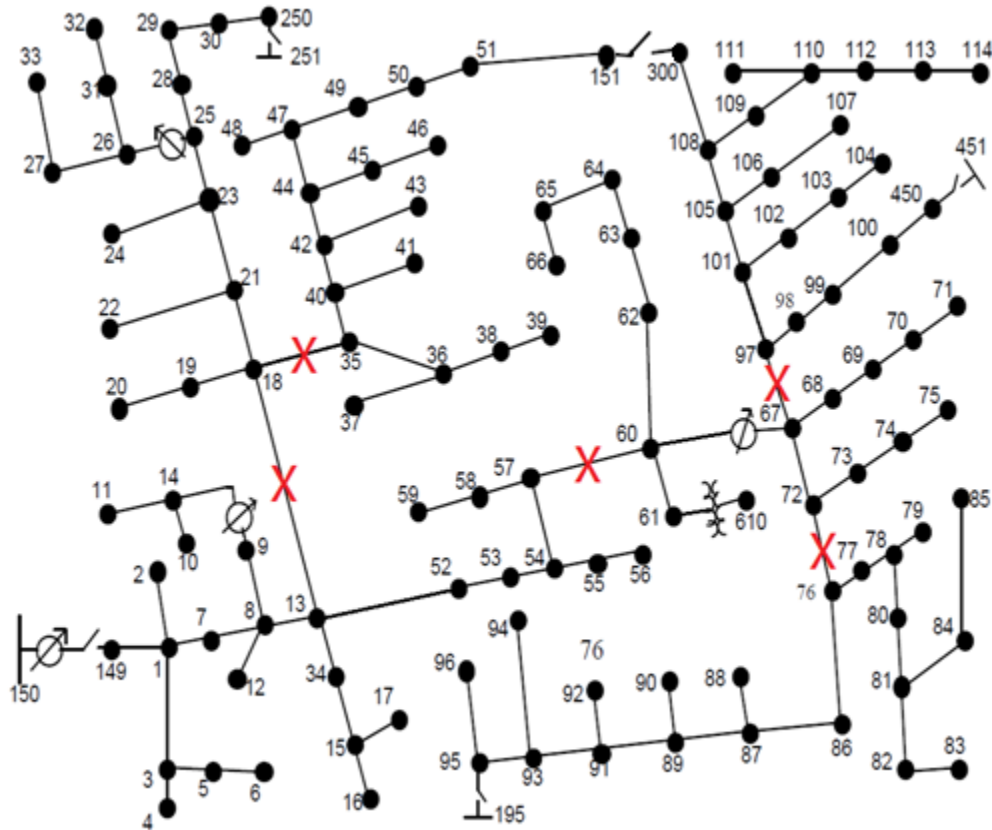


Figure 4.10 Optimal switch locations for 1 year payback period.

### 4.3 Automatic Network Reconfiguration

#### 4.3.1 Rule-based Reconfiguration

Basically, the rule-based reconfiguration is done by finding the switches near to a fault, operating them to isolate the faulted zone and to restore power to unfaulted zone. To increase the efficiency to search for nearest switches, a data tree structure for the power model is constructed by applying the object-oriented programming. The tree structure is updated every iteration of the power model and identifies the network configuration at an iteration. The search algorithm starts searching from the location of fault, which is assumed to be provided by measuring devices. Once the switches nearest

to the fault are identified, the reconfiguration algorithm operates them to isolate the faulted zone and restores power to the other zones as the ideal case that is briefly explained in the previous section.

### Rule-based Reconfiguration Algorithm

The very first step of the rule-based reconfiguration algorithm is to construct a tree data structure. Each node in the network is represented as a struct (short for “structure”). For example, the struct for the node 13 is shown in Figure 4.11.

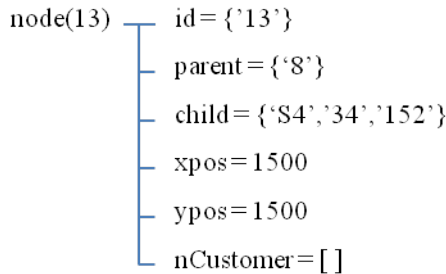


Figure 4.11 Data Structure for Node 13

A node struct has 6 fields: ‘id’, ‘parent’, ‘child’, ‘xpos’, ‘ypos’, and ‘nCustomer’. The fields ‘xpos’ and ‘ypos’ are used to plot the grid. The field ‘nCustomer’ contains the number of customers at a node. The 5 switches are denoted as ‘S1’, ‘S2’, ‘S3’, ‘S4’, and ‘S5’, respectively. The node 149, which is connected to the main feeder (node 150), is considered as a root node for the whole tree data structure. Suppose that there are two nodes, N1 and N2, and that they are connected to each other. If node N1 is closer to Node 150, then the node N1 is a parent of the node N2, and N2 is a child of N1. In this way, all parent-child relationship can be determined because the baseline network is radial. Also, for the radiality to be held, all nodes must have only one parent. If a node has more than one parent, the network would have a loop.

Once a fault occurs, the algorithm first starts to search for the switches nearest to the fault. In order to do this, the algorithm invokes the path-finding routine, which determines the paths of the switches to the fault and also determines the switch commands. An example of the path-finding algorithm is shown in Figure 4.12, where switches S1, S2, S3, and S9 are tie switches, and switches S4 to S8 are automatic switches. The switches are located as shown in Figure 4.13. This example shows that a fault occurs at node 19. The algorithm searches for an upstream path from the fault and terminates the searching process at a node with a switch or at the root node, 149. If there doesn't exist a path from the fault to the root node, in other words, the searching process is terminated at a node with a switch, the fault can be assumed to have occurred somewhere below the switch from the viewpoint of the tree structure. In this example, the searching process is terminated at the switch S4, which indicates that the fault has occurred at the lower level than S4 and that the main feeder can be utilized after the fault is isolated.

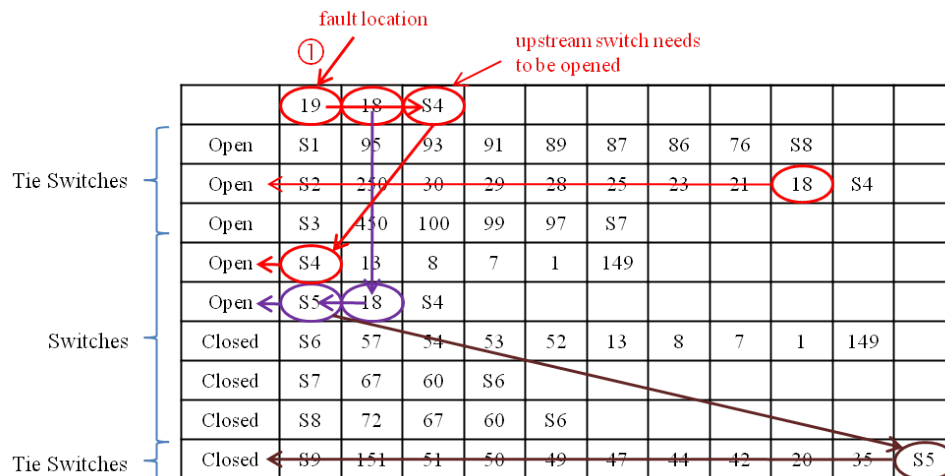


Figure 4.12 Paths finding and switch commands determination

Let the path from the fault to Switch S4 denoted by P0. In case of the switch S5, it has a common node with the path P0, which means that the switch S5 must be opened to isolate the fault. The remaining switches, S6 to S8, are determined to remain closed because they don't have any common node with the path P0. After the switching commands for the automatic switches are determined, the algorithm determines the commands for the tie switches. To avoid a looped network, any two feeders cannot be utilized at the same time. According to the path table, the tie switch S1 has a path to the root node 149, which indicates that S1 cannot be connected to the network. In the same way, the tie switch S3 should remain opened. For the tie switch S2, it has a common node with the path P1 and hence it must also remain opened. For the last tie switch S9, it is connected to the switch S5. Since the switch S5 needs to be opened, the switch S9 should be closed in order to provide power to the area containing nodes 35 to 51.

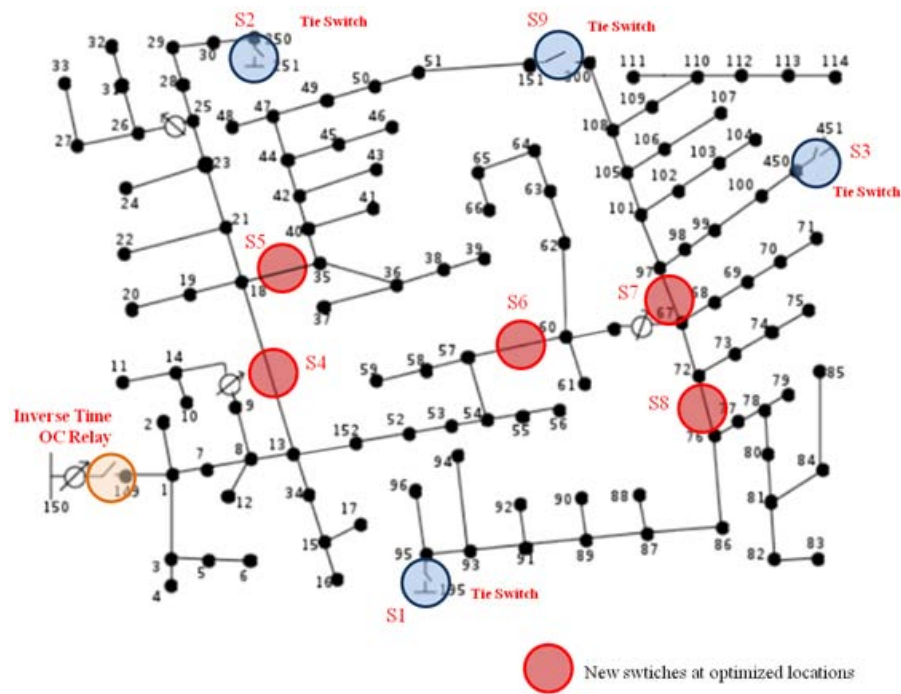


Figure 4.13 Optimal switch locations for automatic reconfiguration

In summary, the algorithm reconfigures the network as follows:

- 1) Identify an upstream path,  $P_0$ , from the fault: ex)  $P_0 = \{ '19', '18', 'S4' \}$
- 2) Set the command for the switch  $S_4$  to 'OPEN': ex)  $SwCmd(S_4) = 0$
- 3) Search for a path from the switches until it reaches the fault or the root node 149 and denote it as  $P_1, P_2, \dots, P_9$ , respectively: ex)  $P_7 = \{ 'S7', '67', '60', 'S6' \}$
- 4) If the path  $P_i$ , where  $i=1, \dots, 9$ , has a common node with the path  $P_0$ , then set the command for the corresponding switch to 'OPEN': ex)  $SwCmd(S_5) = 0$
- 5) If not, set the command to 'CLOSED': ex)  $SwCmd(S_6) = 1$
- 6) If a tie switch has a path to the root node, set the command to 'OPEN': ex)  $SwCmd(S_1) = 0$

Figure 4.14 illustrates how the algorithm reconfigures the network when a fault occurs at the node 19. As explained previously, the switches  $S_4$  and  $S_5$  are opened to isolate the fault, and the switches  $S_6$ ,  $S_7$ , and  $S_8$  remain closed. The tie switches  $S_1$  and  $S_3$  remain open to make the network radial. The tie switch  $S_2$  is opened since it is connected to the faulty area. Finally, the tie switch  $S_9$  gets closed to provide power to the area containing nodes 35 to 51; otherwise, the area loses power so that it degrades the SAIDI index score.

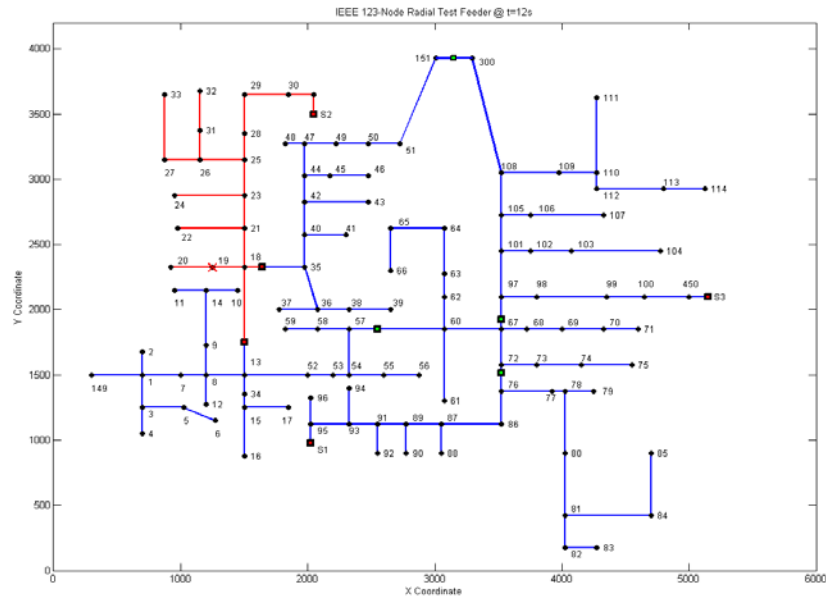


Figure 4.14 Network Plot @ t=12s with a Fault at Node 19

### 4.3.2 Simulation Results of the Optimal Reconfiguration

To verify each reconfiguration technique, 119 fault scenarios are applied over which SAIDI scores are averaged so that SAIDI reductions of each technique can be compared with that of the baseline model that is the one with no automatic switches added. And SAIDI can be improved as high as 82.19%. Table below shows the effect of types of switches on Power system reliability.

Table 4.15 - Effects of Types of Switches on Reliability

No. of Automatic Switches	No. of Manual Switches	Averaged, Best SAIDI Reduction
0	5	0%
2	3	69.65%
3	2	75.86%
4	1	78.07%
5	0	82.19%
5	1	82.94%
5	2	83.27%
5	3	83.78%

## CHAPTER 5

### CONCLUSION AND FUTURE WORK

The work performed in this thesis focused on the reliability enhancement in power distribution systems. An algorithm was built to realize optimal relay setting for several test systems. Both overcurrent relays and distance relays and their coordination were considered in the optimization problem. In addition, fuse saving scheme was applied to avoid long-time power outage.

After the fault occurrence, another algorithm was developed to realize optimal network reconfiguration as quickly as possible to restore as much out-of-service loads as possible. Some optimization technique was applied to find switches to isolate the fault and restore power to non faulted sections via sectionalizing switches and open tie switches. Meanwhile, optimal switch placement algorithm was created to decide the number and location of additional switches to improve the reliability of the system at a reasonable cost.

Preliminary results were obtained from the IEEE 123-Node Test Feeder. The optimization technique can also be used in a realistic distribution system with the combination of AMI and state estimation. For example, a typical distribution system usually has 40 to 50 miles of circuits, or a whole substation usually has 8 to 12 distribution feeders. Advanced metering infrastructure (AMI) will be used to realize a high fidelity real-time monitoring system and a three-phase state estimation algorithm which filters the measurements to give the real-time model of the system. The results of the state estimator are used as an input to the optimization algorithm responsible for generating real-time control signals through which all the available devices will be coordinated to achieve system level optimal operating conditions. In this case, nominal

current can be received from state estimation. Those values will then be transformed into constraints in the optimization problem. According to the weather information, the potential area that might be affected by the severe weather will be determined. Since the location and status of the relays and switches in the area are known in advance, the optimization algorithm will then decide the optimal relay setting and optimal network reconfiguration. With the results from the optimization algorithm, the settings of the relays in the distribution system are updated accordingly and the load break switches and tie switches are operated in sequence through remote control system so that the system can react to the fault the fastest and restore power to as many customers as possible.

## APPENDIX A

### BASIC RELIABILITY CALCULATIONS

System average interruption duration index (SAIDI) is the average duration of all interruptions per utility customer served. It is determined by dividing the sum of all customer interruption durations in a year by the number of customers served.

$$SAIDI = \frac{\text{total duration of sustained outages}}{\text{number of customers served}}$$

System Average Interruption Frequency Index (SAIFI) is the average number of times that a system customer is interrupted during a time period. It is determined by dividing the sum of all customer interruption durations during a year by the number of customers served.

$$SAIFI = \frac{\text{total number of sustained outages}}{\text{number of customers served}}$$

Customer Average Interruption Duration Index (CAIDI) is the average duration of interruptions among those customers experiencing interruptions during a year. It is determined by dividing the sum of all customer interruption durations by the total number of interruptions over 1-year period.

$$CAIDI = \frac{\text{total duration of sustained outages}}{\text{number of sustained outages}}$$

Momentary Average Interruption Frequency Index (MAIFI) is the average number of momentary interruptions that a customer experiences during a year. Electric power utilities may define momentary interruptions differently, with some considering a momentary interruption to be an outage of less than 1 minute in duration while others may consider a momentary interruption to be an outage within several seconds.

$$MAIFI = \frac{\text{number of momentary interruptions}}{\text{number of customers served}}$$

## APPENDIX B

### DESCRIPTION OF THE TEST SYSTEM

Figure B.1 shows the 13.8 KV 123 node test system. The ratings of each of the units are given in the following tables and figures.

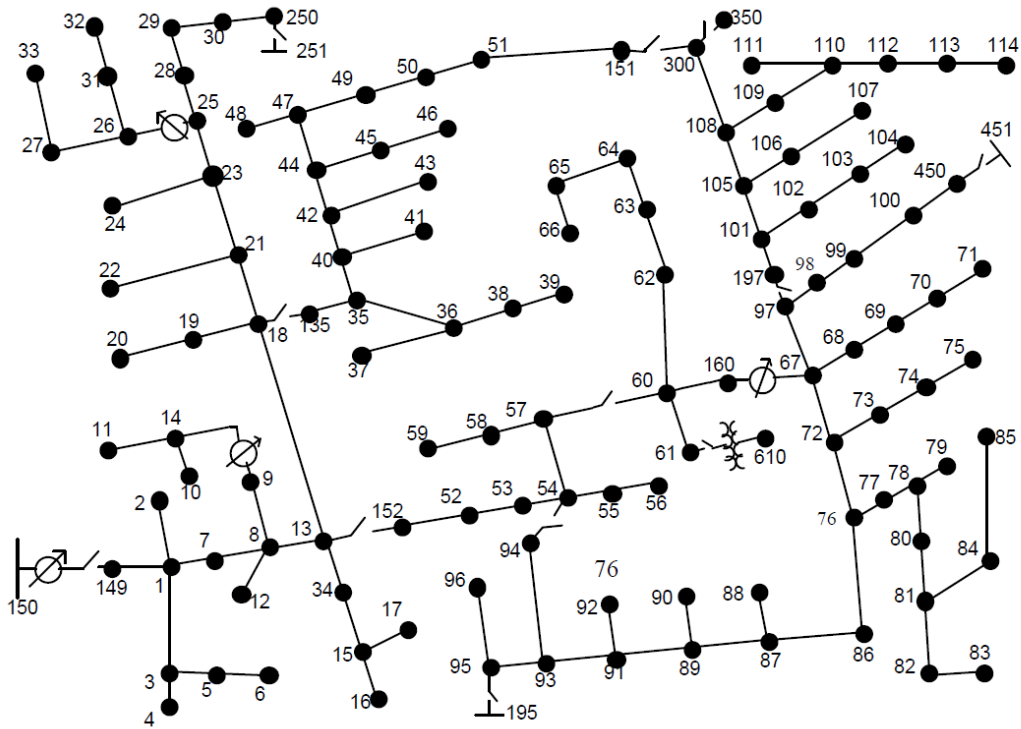


Figure B.1 IEEE 123-Node Test Feeder

Table B.1 Line segment data

Node A	Node B	Length (ft.)	Config.
1	2	175	10
1	3	250	11
1	7	300	1
3	4	200	11
3	5	325	11
5	6	250	11
7	8	200	1
8	12	225	10
8	9	225	9
8	13	300	1
9	14	425	9
13	34	150	11
13	18	825	2
14	11	250	9
14	10	250	9
15	16	375	11
15	17	350	11
18	19	250	9
18	21	300	2
19	20	325	9
21	22	525	10
21	23	250	2
23	24	550	11
23	25	275	2
25	26	350	7
25	28	200	2
26	27	275	7
26	31	225	11
27	33	500	9
28	29	300	2
29	30	350	2
30	250	200	2
31	32	300	11
34	15	100	11
35	36	650	8
35	40	250	1
36	37	300	9
36	38	250	10
38	39	325	10
40	41	325	11
40	42	250	1
42	43	500	10
42	44	200	1
44	45	200	9

42	44	200	1
44	45	200	9
44	47	250	1
45	46	300	9
47	48	150	4
47	49	250	4
49	50	250	4
50	51	250	4
52	53	200	1
53	54	125	1
54	55	275	1
54	57	350	3
55	56	275	1
57	58	250	10
57	60	750	3
58	59	250	10
60	61	550	5
60	62	250	12
62	63	175	12
63	64	350	12
64	65	425	12
65	66	325	12
67	68	200	9
67	72	275	3
67	97	250	3
68	69	275	9
69	70	325	9
70	71	275	9
72	73	275	11
72	76	200	3
73	74	350	11
74	75	400	11
76	77	400	6
76	86	700	3
77	78	100	6
78	79	225	6
78	80	475	6
80	81	475	6
81	82	250	6
81	84	675	11
82	83	250	6
84	85	475	11
86	87	450	6
87	88	175	9
87	89	275	6

Table B.1 continued

89	90	225	10
89	91	225	6
91	92	300	11
91	93	225	6
93	94	275	9
93	95	300	6
95	96	200	10
97	98	275	3
98	99	550	3
99	100	300	3
100	450	800	3
101	102	225	11
101	105	275	3
102	103	325	11
103	104	700	11
105	106	225	10
105	108	325	3
106	107	575	10
108	109	450	9
108	300	1000	3
109	110	300	9
110	111	575	9
110	112	125	9
112	113	525	9
113	114	325	9
135	35	375	4
149	1	400	1
152	52	400	1
160	67	350	6
197	101	250	3

Table B.2 – Three Phase Switches

Three Phase Switches		
Node A	Node B	Normal
13	152	closed
18	135	closed
60	160	closed
61	610	closed
97	197	closed
150	149	closed
250	251	open
450	451	open
54	94	open
151	300	open
300	350	open

Table B.3 – Overhead Line Configuratioions

Overhead Line Configurations (Config.)				
Config.	Phasing	Phase Cond.	Neutral Cond.	Spacing
		ACSR	ACSR	ID
1	A B C N	336,400 26/7	4/0 6/1	500
2	C A B N	336,400 26/7	4/0 6/1	500
3	B C A N	336,400 26/7	4/0 6/1	500
4	C B A N	336,400 26/7	4/0 6/1	500
5	B A C N	336,400 26/7	4/0 6/1	500
6	A C B N	336,400 26/7	4/0 6/1	500
7	A C N	336,400 26/7	4/0 6/1	505
8	A B N	336,400 26/7	4/0 6/1	505
9	A N	1/0	1/0	510
10	B N	1/0	1/0	510
11	C N	1/0	1/0	510

Table B.4 – Underground Line Configuration

Underground Line Configuration (Config.)			
Config.	Phasing	Cable	Spacing ID
12	A B C	1/0 AA, CN	515

Table B.5 – Shunt Capacitors data

Shunt Capacitors			
Node	Ph-A	Ph-B	Ph-C
	kVAr	kVAr	kVAr
83	200	200	200
88	50		
90		50	
92			50
Total	250	250	250

The spacing ID numbers and type for overhead lines are summarized in Table B.6, and Figure B.2 shows the spacing distances between the phase conductors and the neutral conductor for Spacing ID numbers used for the overhead lines.

Table B.6 Overhead Line Spacing

Spacing ID	Type
500	Three-Phase, 4 wire
505	Two-Phase, 3 wire
510	Single-Phase, 2 wire

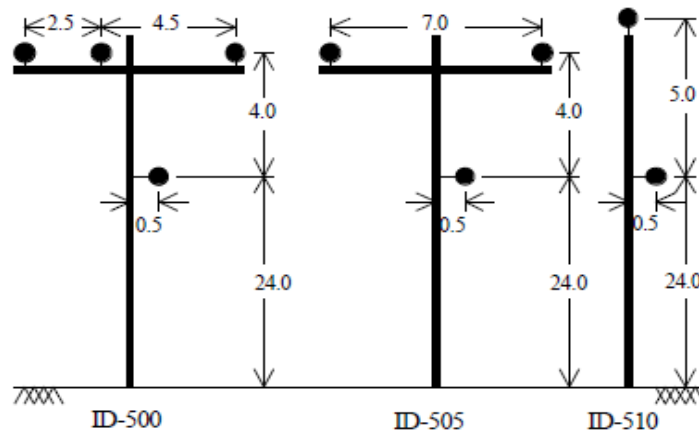


Figure B.2 Overhead Line Spacing

The spacing ID numbers and type for underground lines are summarized in Table B.7, and Figure B.3 shows the spacing distances between cables for underground lines:

Table B.7 Underground Line Spacing

Spacing ID	Type
515	Three-Phase, 3 Cable
520	Single-Phase, 2 Cable

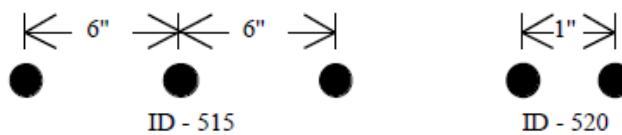


Figure B.3 Underground Line Spacing

Table B.8 Load data

Spot Loads							
Node	Load	Ph-1	Ph-1	Ph-2	Ph-2	Ph-3	Ph-3
	Model	kW	kVAr	kW	kVAr	kW	kVAr
1	Y-PQ	40	20	0	0	0	0
2	Y-PQ	0	0	20	10	0	0
4	Y-PQ	0	0	0	0	40	20
5	Y-I	0	0	0	0	20	10
6	Y-Z	0	0	0	0	40	20
7	Y-PQ	20	10	0	0	0	0
9	Y-PQ	40	20	0	0	0	0
10	Y-I	20	10	0	0	0	0
11	Y-Z	40	20	0	0	0	0
12	Y-PQ	0	0	20	10	0	0
16	Y-PQ	0	0	0	0	40	20
17	Y-PQ	0	0	0	0	20	10
19	Y-PQ	40	20	0	0	0	0
20	Y-I	40	20	0	0	0	0
22	Y-Z	0	0	40	20	0	0
24	Y-PQ	0	0	0	0	40	20
28	Y-I	40	20	0	0	0	0
29	Y-Z	40	20	0	0	0	0
30	Y-PQ	0	0	0	0	40	20
31	Y-PQ	0	0	0	0	20	10
32	Y-PQ	0	0	0	0	20	10
33	Y-I	40	20	0	0	0	0
34	Y-Z	0	0	0	0	40	20
35	D-PQ	40	20	0	0	0	0
37	Y-Z	40	20	0	0	0	0
38	Y-I	0	0	20	10	0	0
39	Y-PQ	0	0	20	10	0	0
41	Y-PQ	0	0	0	0	20	10
42	Y-PQ	20	10	0	0	0	0
43	Y-Z	0	0	40	20	0	0
45	Y-I	20	10	0	0	0	0
46	Y-PQ	20	10	0	0	0	0
47	Y-I	35	25	35	25	35	25
48	Y-Z	70	50	70	50	70	50
49	Y-PQ	35	25	70	50	35	20
50	Y-PQ	0	0	0	0	40	20
51	Y-PQ	20	10	0	0	0	0
52	Y-PQ	40	20	0	0	0	0
53	Y-PQ	40	20	0	0	0	0
55	Y-Z	20	10	0	0	0	0
56	Y-PQ	0	0	20	10	0	0

58	Y-I	0	0	20	10	0	0
59	Y-PQ	0	0	20	10	0	0
60	Y-PQ	20	10	0	0	0	0
62	Y-Z	0	0	0	0	40	20
63	Y-PQ	40	20	0	0	0	0
64	Y-I	0	0	75	35	0	0
65	D-Z	35	25	35	25	70	50
66	Y-PQ	0	0	0	0	75	35
68	Y-PQ	20	10	0	0	0	0
69	Y-PQ	40	20	0	0	0	0
70	Y-PQ	20	10	0	0	0	0
71	Y-PQ	40	20	0	0	0	0
73	Y-PQ	0	0	0	0	40	20
74	Y-Z	0	0	0	0	40	20
75	Y-PQ	0	0	0	0	40	20
76	D-I	105	80	70	50	70	50
77	Y-PQ	0	0	40	20	0	0
79	Y-Z	40	20	0	0	0	0
80	Y-PQ	0	0	40	20	0	0
82	Y-PQ	40	20	0	0	0	0
83	Y-PQ	0	0	0	0	20	10
84	Y-PQ	0	0	0	0	20	10
85	Y-PQ	0	0	0	0	40	20
86	Y-PQ	0	0	20	10	0	0
87	Y-PQ	0	0	40	20	0	0
88	Y-PQ	40	20	0	0	0	0
90	Y-I	0	0	40	20	0	0
92	Y-PQ	0	0	0	0	40	20
94	Y-PQ	40	20	0	0	0	0
95	Y-PQ	0	0	20	10	0	0
96	Y-PQ	0	0	20	10	0	0
98	Y-PQ	40	20	0	0	0	0
99	Y-PQ	0	0	40	20	0	0
100	Y-Z	0	0	0	0	40	20
102	Y-PQ	0	0	0	0	20	10
103	Y-PQ	0	0	0	0	40	20
104	Y-PQ	0	0	0	0	40	20
106	Y-PQ	0	0	40	20	0	0
107	Y-PQ	0	0	40	20	0	0
109	Y-PQ	40	20	0	0	0	0
111	Y-PQ	20	10	0	0	0	0
112	Y-I	20	10	0	0	0	0
113	Y-Z	40	20	0	0	0	0
114	Y-PQ	20	10	0	0	0	0
Total		1420	775	915	515	1155	635

Figure B.4 shows the 123 node test system built in WinIGS-F. Besides the parameters listed above, for adaptive relay programming, there are additional equipments in the system such as relays and fuses. Detailed information about those equipments are shown in Table B.9.

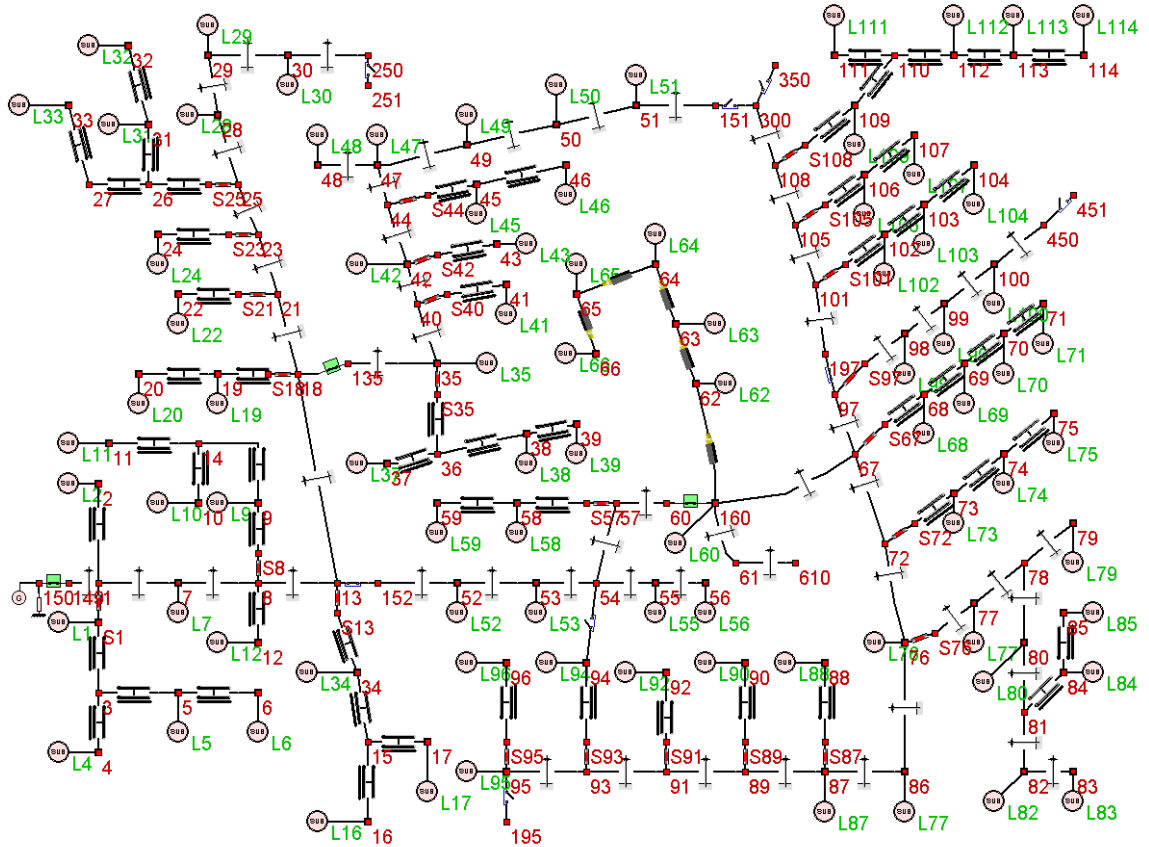


Figure B.4 IEEE 123-Node Test Feeder in WinIGS - F

Table B.9 Switch type and location in the test system

Node A	Node B	Type	Norminal current	Fuse Rating
1	S1	Fuse	14.1	25
8	S8	Fuse	13.5	25
13	S13	Fuse	13.9	25
18	S18	Fuse	10.7	25
18	135	Recloser	30.3	
21	S21	Fuse	5.7	12
23	S23	Fuse	5.5	12
25	S25	Fuse	5.5	12
35	S35	Fuse	5.6	12
40	S40	Fuse	2.8	6
42	S42	Fuse	5.7	12
44	S44	Fuse	5.4	12
57	S57	Fuse	5.6	12
60	160	Recloser	65	
67	S67	Fuse	15.7	25
72	S72	Fuse	16.3	25
76	S76	Fuse	11	25
87	S87	Fuse	5.2	12
89	S89	Fuse	5.5	12
91	S91	Fuse	5.5	12
93	S93	Fuse	5.2	12
95	S95	Fuse	2.8	6
97	S97	Fuse	5.5	12
101	S101	Fuse	14	25
105	S105	Fuse	11.1	25
108	S108	Fuse	18.1	25
149	150	Breaker	160	

In order to calculate SAIDI and MAIFI scores as accurately as possible, each load in the system needed to be assigned a set of customers. Looking at the customer data for the U.S. given in the EIA's (8), the following observations can be seen:

- 1) 37%, 36%, and 27% of the U.S. electricity load belongs to residential, commercial, and industrial customers, respectively

- 2) 87%, 12%, and 1% of the U.S. electricity customers are residential, commercial, and industrial customers, respectively
- 3) The average industrial load is about 120 times larger than the average residential load
- 4) The average commercial load is about 7 times larger than the average residential load

Additionally, the following assumptions were made regarding the IEEE 123 node model:

- 1) Industrial customers can only be located at 3-phase lines, and are generally segregated from regular residential/commercial sectors.
- 2) The average residential load is 1.67 kW and 0.83 kVar

Using these guidelines, a unique customer profile of 878 customers was created for our 123 node model, with 764 of the 878 customers being residential, 109 being commercial, and 5 being industrial. Detailed information about the load profile is shown in Table B.10.

Table B.10 Load data in the test system

Node	Residential load	Commercial load	Industrial load	Number of customer
1	12	1.71	0	13.71
2	6	0.86	0	6.86
4	12	1.71	0	13.71
5	6	0.86	0	6.86
6	12	1.71	0	13.71
7	6	0.86	0	6.86
9	12	1.71	0	13.71
10	6	0.86	0	6.86
11	12	1.71	0	13.71
12	6	0.86	0	6.86
16	12	1.71	0	13.71
17	6	0.86	0	6.86
19	12	1.71	0	13.71

Table B.10 Continued

20	12	1.71	0	13.71
22	12	1.71	0	13.71
24	12	1.71	0	13.71
28	12	1.71	0	13.71
29	12	1.71	0	13.71
30	12	1.71	0	13.71
31	6	0.86	0	6.86
32	6	0.86	0	6.86
33	12	1.71	0	13.71
34	12	1.71	0	13.71
35	12	1.71	0	13.71
37	12	1.71	0	13.71
38	6	0.86	0	6.86
39	6	0.86	0	6.86
41	6	0.86	0	6.86
42	6	0.86	0	6.86
43	12	1.71	0	13.71
45	6	0.86	0	6.86
46	6	0.86	0	6.86
47	1.48	0.21	0.5	2.19
48	2.95	0.42	1	4.38
49	1.97	0.28	0.67	2.92
50	12	1.71	0	13.71
51	6	0.86	0	6.86
52	12	1.71	0	13.71
53	12	1.71	0	13.71
55	6	0.86	0	6.86
56	6	0.86	0	6.86
58	6	0.86	0	6.86
59	6	0.86	0	6.86
60	6	0.86	0	6.86
62	12	1.71	0	13.71
63	12	1.71	0	13.71
64	1.05	0.15	0.36	1.56
65	1.97	0.28	0.67	2.92
66	1.05	0.15	0.36	1.56
68	6	0.86	0	6.86
69	12	1.71	0	13.71
70	6	0.86	0	6.86
71	12	1.71	0	13.71
73	12	1.71	0	13.71
74	12	1.71	0	13.71
75	12	1.71	0	13.71

Table B.10 Continued

76	3.45	0.49	1.17	5.11
77	12	1.71	0	13.71
79	12	1.71	0	13.71
80	12	1.71	0	13.71
82	12	1.71	0	13.71
83	6	0.86	0	6.86
84	6	0.86	0	6.86
85	12	1.71	0	13.71
86	6	0.86	0	6.86
87	12	1.71	0	13.71
88	12	1.71	0	13.71
90	12	1.71	0	13.71
92	12	1.71	0	13.71
94	12	1.71	0	13.71
95	6	0.86	0	6.86
96	6	0.86	0	6.86
98	12	1.71	0	13.71
99	12	1.71	0	13.71
100	12	1.71	0	13.71
102	6	0.86	0	6.86
103	12	1.71	0	13.71
104	12	1.71	0	13.71
106	12	1.71	0	13.71
107	12	1.71	0	13.71
109	12	1.71	0	13.71
111	6	0.86	0	6.86
112	6	0.86	0	6.86
113	12	1.71	0	13.71
114	6	0.86	0	6.86

## REFERENCES

- [1] Richard E. Brown, "Impact of Smart Grid on distribution system design," Power and Energy Society General Meeting, pp. 1-4, July 2008
- [2] A. J. Urdaneta, R. Nadira, and L. G. Perez, "Optimal Coordination of Directional Overcurrent Relays in Interconnected power Systems," IEEE Transactions on Power Delivery, vol. 3, pp. 903-911, July 1988.
- [3] A.P. Sakis Meliopoulos and George J. Cokkinides, Power System Relaying, Theory and Applications, 1996
- [4] B. Chattopadhyay, M. S. Sachdev, and T. S. Sidhu, "An on-line relay coordination algorithm for adaptive protection using linear programming technique," IEEE Trans. Power Delivery, vol. 11, pp. 165-173, Jan. 1996.
- [5] A. J. Urdaneta, H. Restrepo, S. Marquez, and J. Sanchez, "Coordination of Directional Overcurrent Relay Timing Using Linear Programming technique," IEEE Transactions on Power Delivery, vol. 11, pp. 122-129, Jan. 1996.
- [6] Juan M. Gers and Edward J. Holmes, Protection of Electricity Distribution Networks, The Institution of Electrical Engineers, London, United Kingdom, 2004, pp.70-73
- [7] Perez, L. G., Urdaneta, A.J., "Optimal Computation of Distance Relays Second Zone Timing in a Mixed Protection Scheme with Directional Overcurrent Relays," IEEE Trans. On Power Delivery, vol. 16, NO. 3, pp. 385-388, July 2001
- [8] Vanderplaats, Garret N. Numerical Optimization Techniques for Engineering Design. Colorado Springs : VR&D, 2005..
- [9] Venter, Gerhard and Sobieski, Jaroslaw., Particle Swarm Optimization, 2003, AIAA, pp. 1583-1589.
- [10] R. C. and Shi, Y., Comparing Inertia Weights and Constriction Factors in Particle Swarm Optimization. Eberhart, IEEE. pp. 84-88, 2000.
- [11] Clerc, M., The Swarm and the Queen: Towards a Deterministic and Adaptive Particle Swarm Optimization. Washington, D.C., Proc. 1999 ICEC. pp. 1951-1957.
- [12] Zhang, Li-ping, Yu, Huan-jun and Hu, Shang-xu., Optimal Choice of Parameters for Particle Swarm Optimization, Journal of Zhejiang University Science, pp. 528-534, 2005
- [13] Mithulananthan, N., Oo, Than and Phu, Le Van., Distributed Generator Placement in Power Distribution System Using Genetic Algorithm to Reduce Losses., Thammasat Int. J. Sc. Tech., Vol. 9, No. 3. pp. 55-62, 2004.

- [14] Grefenstette, John J., Optimization of Control Parameters for Genetic Algorithms, IEEE Trans. on Systems, Man, and Cybernetics, Vol. SMC-16, No. 1. pp. 122-128,1986.